

ABSTRACT

SUN, JING. Optimization of the Neutron Absorption Steady Source Measurement Method --by using an ^{124}Sb -Be Source. (Under the direction of Robin P. Gardner.)

In the mineral exploration and oil well logging industries where logging tools are used based on neutron moderation and absorption principles, one needs to have an accurate knowledge of the neutron absorption cross-sections of the sample of interest for calibration purposes. This is difficult to ascertain by ordinary chemical analysis since some elements that are present in trace amounts (like boron, samarium, and gadolinium) have very large neutron absorption cross-sections. In oil well logging applications, chlorine appears in larger than trace amounts and often dominates the absorption cross-sections. For this reason a sensitive measurement is obtained by using the response to a source of thermal neutrons when a small sample is placed within a good moderating medium. Tittle and Crawford (1983) described and demonstrated such an approach. This method has evolved into one that uses a ^{252}Cf source of neutrons with a ^3He proportional counter. Attempts to optimize the sensitivity of this technique by Monte Carlo simulation with both MCNP and a specific purpose Monte Carlo code (Mickael, 1988) involving different detector positions relative to the sample, variable source-to-sample distances, and different moderators (Bussian, Jetter, and Supernaw, 1991, Talavarjula, 1995, and Sood, Gardner, and Gray, 2000) have had only limited success. The present approach involves the use of a ^{124}Sb -Be neutron source with an average neutron energy of about 12 Kev compared to the 3 to 4 MeV average of the ^{252}Cf source. Monte Carlo calculations with MCNP and subsequent benchmark experiment indicate a much improved sensitivity and accuracy with the ^{124}Sb -Be source.

**Optimization of the Neutron Absorption Steady
Source Measurement Method
--by using an ^{124}Sb -Be Source**

by

JING SUN

Master's Thesis submitted to the Faculty of
North Carolina State University
in partial fulfillment of
the requirements for the degree of
Master of Science

NUCLEAR ENGINEERING

Raleigh, North Carolina

2002

APPROVED BY:

Minor representative

Co-Chair of Advisory Committee

Chair of Advisory Committee

BIOGRAPHY

Jing Sun was born in Jilin, China on February 28th, 1976 and moved to Beijing when she was one and a half years old. In the fall of 1994, she began her college education in Tsinghua University and obtaining her Bachelor of Science degree in Engineering Physics in the summer of 1999.

In August 2000, the author was admitted to North Carolina State University as a doctoral student in the Department of Nuclear Engineering. During the first two semesters, she was supported by the Department. For the remainder of her work, she was supported by the Center for Engineering Applications of Radioisotopes as a research assistant.

Jing Sun is the daughter of Zhongzhi Sun and Guirong Liu. She is the only child in the family.

ACKNOWLEDGEMENTS

First of all, I would like to record my deep indebtedness and my sincere gratitude to the chairman of my advisory committee, Professor Robin P. Gardner for the valuable guidance, support and continuous encouragement he gave me during the research. I am also equally indebted to the co-chairman of the committee, Professor Charles W. Mayo, for his helpful advice and suggestions. Special thanks are also extended to Dr. Wushow Chou, the minor representative, for his suggestions and attendance.

I would gratefully acknowledge the contribution of Lecturer and Reactor Health Physicist, Dr. Gerald D. Wicks, for the computational procedure and benchmark of the source activation safety also the design of capsulation of Antimony pellet. I am grateful to Larry Dufour and other technicians in Workshop for their carefully design and efforts for the experimental device and the source capsulation. I am also grateful to all group members of CEAR, SangHoon Lee, Walid Metwally, Weijun Guo, Xiaogang Han and Ashraf Shehata, who have inspired and assisted in my research study. I would also gratefully acknowledge the financial support of the Associates Program for Nuclear Techniques in Oil Well Logging with present members Baker Atlas and Advantage Engineering.

Finally I would like to extend my sincere gratitude to my parents for their always moral support from far away in my home country China. For my boyfriend, Dapeng, I would like to thank him for his patience, understanding and moral support.

Contents

List of Tables	vii
-----------------------	------------

List of Figures	viii
------------------------	-------------

1 Introduction	1
1.1 An Overview	1
1.2 Cross Section Experiment	1
1.3 Literature Review	2
1.3.1 Tittle and Crawford's work	2
1.3.2 Salaita's work	2
1.3.3 Bussian, Jetter and Supernaw's work	3
2 Experimental Technique	4
2.1 Experimental principle and method	4
2.2 Previous Work at NCSU	6
2.2.1 Tallavarjula's work	6
2.2.2 Sood's work	6
2.3 The Improved Design	7
3 MCNP Simulation	9
3.1 A brief description of the input file	10
3.1.1 Cell Cards	11

3.1.2	Surface Cards	11
3.1.3	Material Cards and Perturbation Effect	12
3.1.4	Importance Cards	13
3.1.5	Source Specification Cards	13
3.1.6	Tally Specification Cards	13
3.1.7	Weight Windows	14
3.1.8	Peripheral Cards	15
3.2	Simulations with MCNP	15
3.2.1	Calculation with Aqueous Samples	16
3.2.2	Calculation with Powder Samples	17
3.3	Discussions of Simulation	22
4	Experiments with $^{124}\text{Sb-Be}$ Source	24
4.1	Experiment System	24
4.2	Counting Rate Electronics	25
4.3	Preparation for Samples	30
4.3.1	Aqueous Samples	30
4.3.2	Powder Samples	31
4.4	Preparation for Source	32
4.5	Calibrations with Standard Samples	37
4.5.1	Experiments with ^{252}Cf and $^{124}\text{Sb-Be}$ Source in new apparatus	37
4.5.2	Semi-empirical model	40
4.5.3	Compare to previous work (^{252}Cf Source in paraffin box)	41

4.6 Discussions for Experiment Measurements	49
5 Conclusions and Future work	51
5.1 Summary and Conclusions	51
5.2 Future Work	52
Reference	54
Appendix	56
A MCNP INP file	56
B Style and model of electronic apparatus	60
C Pictures For Sb(Be) Source Experiment	61
D Procedure for test of a Sb(Be) source	62
E Procedure for use a Sb(Be) source	66
F Calculation for Source Mass	67
G Calculation for Source Activation Time	68

List of Tables

Table 3-1 Data from simulations of Both Antimony-Beryllium and Californium steady source with sodium chloride solution samples	19
Table 3-2 Data from simulations of Both Antimony-Beryllium and Californium steady source with silicon oxide and boric acid powder samples	19
Table 3-3 Sensitivity improvement--The comparison for slopes and intercepts of the calibration curves between two sources	23
Table 4-1. The thermal neutron microscopic cross sections (2200 m/s) for pure element as standard aqueous and powder samples	34
Table 4-2. The pre-calculated macroscopic cross sections of standard aqueous samples	35
Table 4-3. The pre-calculated macroscopic cross sections of standard powder samples	36
Table 4-4. Repeated experiments data versus Sood's results	41
Table 4-5. Sensitivity improvement with ^{124}Sb -Be source compare to ^{252}Cf source	50

List of Figures

Figure 2-1. Expected result of sensitivity improvement with ^{124}Sb -Be source	5
Figure 2-2. Design of the steady source technique of cross section measurement	8
Figure 3-1. Sensitivity comparison from simulations of Both Antimony-Beryllium and Californium steady source with sodium chloride solution samples	20
Figure 3-2. Sensitivity comparison from simulations of Both Antimony-Beryllium and Californium steady source with silicon oxide and boric acid powder samples	21
Figure 4-1. Side view of the experiment device	27
Figure 4-2. The electronic circuit system for cross section measurement	28
Figure 4-3. The operating high voltage plateau determination	29
Figure 4-4. The structure of the source encapsulation	33
Figure 4-5. Sensitivity improvement comparison from experiment measurements for absorption cross section between two sources with aqueous samples (90°)	38
Figure 4-6. Sensitivity improvement comparison from experiment measurements for absorption cross section between two sources with aqueous samples (180°)	39
Figure 4-7. Semi-empirical Model of Absorption cross section measurement for both 90° and 180° detector locations by MCNP simulations	43
Figure 4-8. Comparison between MCNP simulation and experimental measurements with ^{124}Sb -Be source	44
Figure 4-9. Detector response with Semi empirical Model (90°)	45

Figure 4-10. Detector response with Semi empirical Model (180°)	46
Figure 4-11. Calibration Curve of Repeat Experiments with ²⁵² Cf Source and paraffin box device	47
Figure 4-12. Comparison between results of Antimony source in water tank and Californium source in paraffin box	48
Figure B-1. Electronic apparatuses for experiment	60
Figure C-1. Experimental device	61
Figure C-2. Aqueous Samples for experiment	61
Figure E-1. Outer Aluminum Capsule and End Caps (left) & Inner Stainless Steel (right) Capsule	66
Figure E-2. Outer Aluminum Capsule and End Caps (top) & Inner Stainless Steel (bottom) Capsule	66
Figure E-3. Figure E-3. End View of Inner Stainless Steel Capsule	66
Figure E-4. Assembled Source	66

Chapter 1

Introduction

1.1 An Overview

In geological industry, like mineral exploration and oil well logging, knowledge of the elements in the formation is very important. Thermal neutron absorption cross sections of the geological materials are vital parameters that are required for modeling neutron porosity logging tool responses. Thus accurate thermal neutron absorption cross sections are significant for proper quantitative interpretation. Generally, rocks in the field would contain trace amounts of some elements like boron, lithium or gadolinium, which have high absorption cross sections. This small variation can bring huge uncertainty. Chemical analysis can often have difficulties and is always expensive. Therefore nuclear cross section evaluation is important in this field. An alternative method for calculating the absorption cross section for using elemental analysis is to measure the thermal neutron cross section directly from the sample.

1.2 Cross Section Experiment

A steady source in a moderating medium has been used to determine thermal neutron cross sections by some previous researchers. The present research is based on those previous works but gains a new optimized design. In this optimized design, a ^{124}Sb -Be source is introduced. Together with a ^3He detector and a sample, they are immersed in a big moderating (water) tank. The change in thermal neutron flux due to the different

samples is calibrated to estimate the absorption cross sections of the sample as measured by the detector. Change in the detector response this is an indirect method. The experiment can be optimized using calculated results from MCNP. In this work Monte Carlo simulation using MCNP is used to study possible improvement of sensitivity of these measurements. In this work the experiment is modified using the information gained by Monte Carlo analyses and benchmarked against the result of the MCNP code. The goal of the thesis is to improve the sensitivity of the experimental measurement of thermal neutron cross section we in the interpretation of oil well logging.

1.3 Literature Review

For the cross section measurement of bulk samples, several experimental techniques have been developed by using steady neutron source methods, there include pulsed neutron source methods and reactivity balance methods. The present work chooses to use a steady neutron source, a sample and a neutron detector immersed in water moderator.

1.3.1 Tittle and Crawford's work

Tittle and Crawford^[1] (1983,1984) introduced the steady neutron source by using a water drum together with a one curie $^{239}\text{Pu-Be}$ neutron source. The rock powders were saturated with water as the samples. The neutron detector was a small ^3He proportional counter. The conclusion was that the effect of scattering by the sample was minimized by using an angle of detector orientation of 90° .

1.3.2 Salaita's work

Salaita^[2]'s (1985) device consisted of a water tank, a ^{252}Cf source and a ^3He detector (1/4" \times 2" in size). The sample material was in a cylindrical plexiglass container. The detector was located very close to the sample and the source was placed at the center of the sample. They tried both the aqueous and the powder samples. Counting times are 200 seconds for each.

1.3.3 Bussian, Jetter and Supernaw's work

Bussian, Jetter and Supernaw^[4]'s (1991) experimental equipment also used a ^{252}Cf source but with two ^3He detectors (0.64 cm in diameter and 7.62 cm in length). The detectors made 180° and 90° angular orientations respectively. The source-sample distance was 17 cm. They obtained both transport and absorption cross sections. Counting rates at 180° and 90° were expressed as linear functions of Σ_a and Σ_{tr} .

Chapter 2

Experimental Technique

2.1 Experimental principle and method

This work is using steady neutron source technique with a ^{124}Sb -Be source, a ^3He detector and a sample immersed in a big moderating (water) tank. The principle for this method is simple and easy to be understood. When a steady neutron source is presented in a large moderating medium, there is an equilibrium established between the neutrons being born and those lost by absorption and leakage. If a sample with a neutron absorption cross section that is different from that of moderating media, is introduced into this system, the neutron flux in the vicinity of the sample will be perturbed. By measuring this change in flux (the change in counts from the detector) due to the presence of a particular sample, it is possible to obtain a calibration for sample cross sections.

Using small sample volume is feasible for geologic rock samples. However, the measurement sensitivity drops with reducing volumes. From Tallavarjula^[5]'s sensitivity studies for different sample volumes by using McDNL code, the sensitivity of the measurement can be expressed as the slope of the linear function of counting rates versus absorption cross sections. If there are two points, a and b, on the calibration result chart (Figure 2-1), r and Σ_a stands for the normalized counting rates and the absorption cross sections, the sensitivity is given by,

$$S = \frac{(Ra - Rb)}{\Sigma_a - \Sigma_b}$$

The sensitivity improvement would be gained by sharper slope of the calibration linear function. From Tallavarjula^[5]'s conclusion, a sample volume in the range (250 cm³ to 300 cm³) should give reasonable sensitivity.

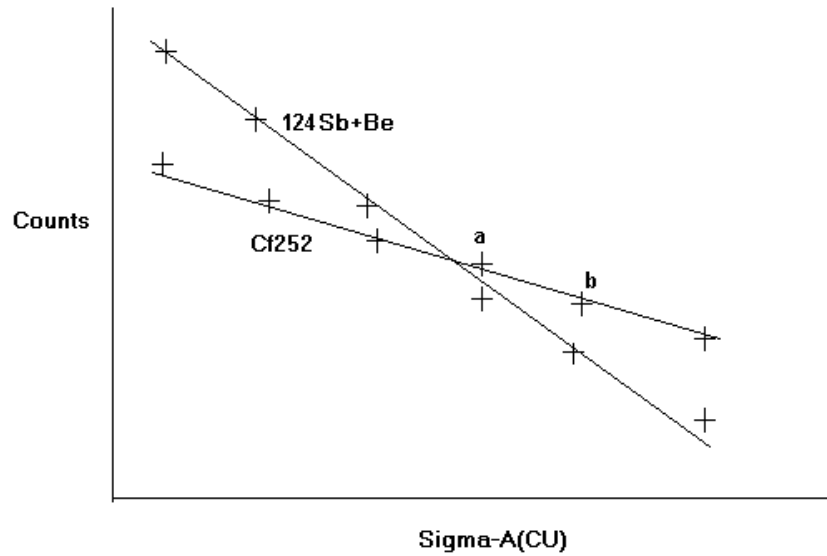


Figure 2-1 Expected result of sensitivity improvement with ¹²⁴Sb-Be source

2.2 Previous work at NCSU

Several experiments using steady source technology have been developed and evaluated at NCSU. These experiments were benchmarked, investigated and developed using Monte Carlo simulation codes, MCNP or McDNL.

2.2.1 Tallavarjula's work

Tallavarjula^[5]'s (1995) work optimized the previous investigations. A water tank, a ^{252}Cf source and a polyethylene sample holder being held immersed in the water moderator. After some Monte Carlo simulations, one of primary design parameters, the source to sample distance, was determined for 15.24 cm. And the sample volume was 275 cm^3 according to the sensitivity. His work counted for both scattering and absorption cross sections by the samples. The effect of scattering on the detector located at 180° was found to be substantial compared to the one located at 90° . Advantage was taken of this fact and a semi-empirical model incorporating both absorption and scattering was developed. Sensitivity was expressed as a function of fractional powder volumes, so that the technique can be used for rock samples available in small amounts.

2.2.2 Sood's work

Sood^[6] (2000) made the experiment device much smaller, the moderator was changed to solid paraffin to reduce the size of the device without large changes in the moderating properties. This can also provide a relatively stable and permanent device and can improve the reproducibility. A larger sample volume (1 liter) was also introduced as well

as the 275 ml one. The ^3He detector was placed at two different angular locations, 180° and 90° . His work improved in the calibration of the device and increased the absorption and scattering cross sections range. Accurate results were obtained relating Σ_a to the detector yield for reference samples of dry powders and aqueous solutions. A semi-empirical model was developed and successfully tested that describes both absorption and scattering cross sections of the sample.

2.3 The improved design

Monte Carlo sensitivity studies demonstrated that neutrons reaching the sample interface should consist of a large fraction of thermal neutrons. To improve the sensitivity of the previous work, a new source ($^{124}\text{Sb-Be}$) has been introduced and a prototype apparatus has been constructed. A $^{124}\text{Sb-Be}$ source with low energy of 23 KeV was used to improve the sensitivity. A water tank was adopted as moderated medium to provide experimental flexibility. The ^3He detectors were placed at 90° and 180° orientation for neutron absorption measurements. The design of the new experimental system is shown below in Figure 2-2.

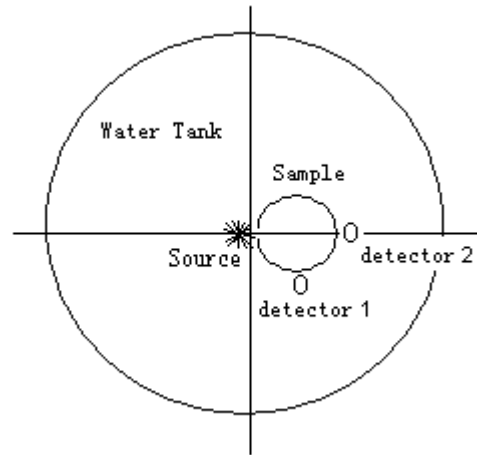


Figure 2-2 Design of the steady source technique of cross section measurement

Chapter 3

MCNP Simulation

To optimize the determination of the experiment parameters and the design of the device, the steady source experiment measurement was simulated using Monte Carlo code: MCNP. MCNP is a general purpose Monte Carlo Neutral Particle transport code, developed at Los Alamos National Laboratory (LANL). One of the many strong points of MCNP is its ability to model the geometries and particle transport in difficult problems nearly exactly. The experiment was benchmarked against the Monte Carlo calculations and then studies. The completed experimental device is depicted in MCNP input file. The system is divided into small cells in order to increase the importance of different positions. The sample was located in the high flux region, as close as possible to the low energy Antimony-Beryllium source. Because of the large gradient in the thermal flux in the region near the source, the detected counting rates are highly sensitive to the detector position. Any small disturbance in the detector location will bring poor reproducibility. Therefore the weight window method and the perturbation effect are also introduced into present research. The MCNP simulated calculations were run on the workstations with UNIX operation system: ULTRA 10. The running time is about one hour. The total history is 10 million for each calculation. MCNP used in present work is available from Los Alamos. The main reference is *MCNP – a general purpose Monte Carlo n-particle transport code version 4C^[10]*. Some features of MCNP input file relevant to the present

experiment and some details of present Monte Carlo work can be discussed in this chapter. A sample input file is included in Appendix-A.

3.1 A brief description of the input file

MCNP stands for Monte Carlo Neutral Particle transport code. It can be used in several transport modes: neutron only, photon only, electron only, combined neutron/photon transport where the photons are produced by neutron interactions, neutron/photon/electron, photon/electron, or electron/photon. The neutron energy regime is from 10^{-11} MeV to 20 MeV. MCNP uses continuous-energy nuclear and atomic data libraries. The primary sources of nuclear data are evaluations from the Evaluated Nuclear Data File (ENDF) system, the Evaluated Nuclear Data Library (ENDL) and the Activation Library (ACTL) compilations from Livermore, and evaluations from the Applied Nuclear Science (T- 2) Group at Los Alamos. The data for cross section calculation in present experiment simulation are selected from library ENDF. According to some preliminary calculations, the source does not work well if the source-sample distance larger than 1 cm. To gain good results, the sample was placed as close as possible to the source. From Tallavarjula^[5]'s work, the volume of the sample was selected as 275 cm³. The calculation time for each sample is about one hour, which means there are 10 million histories in each calculation. Perturbation effect is treated to reduce thermal effect. Thermal $S(\alpha,\beta)$ tables are appropriate if the neutrons are transported at sufficiently low energies where molecular binding effects are important. Thermal $S(\alpha,\beta)$ tables are not required, but they are absolutely essential to get correct answers in problems involving neutron thermalization. The data on these tables

encompass those required for a complete representation of thermal neutron scattering by molecules and crystalline solids. Weight window method is also used as variance reduction technique to control particle weight. More details about weight windows are given in 3.1.7. The cards of MCNP input file relevant to the present experiment are discussed. A complete description of the code can be found in the MCNP manual.

3.1.1 Cell Cards

The entire experiment device is depicted completely. The whole system is divided into small cells in order to get better importance distribution for different positions. For each cell the cell material number, mass density (with a negative sign), Boolean geometry specifications are given. The Boolean specification describes how a certain cell is formed, whether it is inside a surface (prescribed by a preceding “-“ sign) or outside, if it is union of different cells (prescribed by a “:”) or an intersection (a blank). The last line represents void around the system, with a 0 for material number and no density specification. In present experiment, this region stands for the whole space outside the big plexiglass water tank.

3.1.2 Surface Cards

Several surfaces that are used to construct the cells are specified each by a surface number, Mnemonic, and geometry parameters. The surfaces used are planes normal to the principal axes (PX, PY, PZ); spheres with center at origin or any of the axes (SO, SX, SY, SZ); cylinders parallel to the principal axes (C/X, C/Y, C/Z). The planes used in present experiment describe the top and the bottom level of sample, detector, water and

water tank. The cylinders used in present experiment define the sides of the sample, the detector and the water tank. The geometry parameters include intercepts of the planes, and radii for spheres and cylinders.

3.1.3 Material Cards and Perturbation Effect

There are specified by a material number (Mm-card) followed by the cross section file ZAID for each element and its weight fraction. The cross section data is specified by the file rmccs and file tmccs1, which contain the required paths to access the cross section data files. Each material number corresponds to the relative cell number. Material one stands for cell one, moderator medium. Material two stands for powder and aqueous samples. Material three stands for ^3He detector. Mode N stands for thermal neutrons in present experiment.

For thermal neutron scattering from water, the perturbation effect is introduced. $S(\alpha, \beta)$ is specified in the present experiment. The large gradient in the thermal flux is significant in the region near the source, thus the detected count rates are highly sensitive to the detector. Any small disturbance in the detector location will bring poor reproducibility. In general, $S(\alpha, \beta)$ effects are most significant below 2 eV so that their applications are important for thermal neutrons. The $S(\alpha, \beta)$ treatment is invoked by identifiers on MTn cards by the card – *mtn lwtr*. The n refers to the material n defined on a regular Mm card. In the present experiment $S(\alpha, \beta)$ is set for moderation medium water. The appearance of an MTn card will cause the loading of the corresponding $S(\alpha, \beta)$ data from the thermal data file. Because there is no mixing of the two treatments for the same ZAID in the same

material at a given energy, if perturbation effect is introduced, the S (α , β) treatment will automatically override the default or old treatments. The currently S (α , β) contributions to detectors are approximate.

3.1.4 Importance Cards

The importance of a cell is used to terminate the particle's history, for geometry splitting and Russian roulette to help particles move to more important regions of the geometry. Importance for each cell is specified using the card – *imp:n*. In present experiment simulation, assume no neutron particles escape from the water tank by set the zero importance for the cell outside the water tank.

3.1.5 Source Specification cards

The *sdef* card specifies the source coordinates and the cell in which it is located. The energy spectrum specified by *SPn* cards and *SIn* cards and using the built-in functions for source probability. If the surface source is transformed into several locations, the *SIn* card lists the transformation numbers and the *SPn* and *SBn* cards give the probabilities and bias of each transformation. In present simulation the antimony source is specified as a uniform source with the maximum energy 0.023 MeV. For result comparison between two sources, the ^{252}Cf source is also defined in MCNP input file. The parameters [-3 a b] specify Watt fission spectrum for ^{252}Cf source, where a equals 1.025 MeV, b equals 2.926 MeV⁻¹.

3.1.6 Tally Specification Cards

Point detector ^3He is specified by f4:n card and fm4:n card in the present experiment, and the coordinates of the location and radius of sphere of exclusion. The ^3He detector tally calculates the flux passing through the whole detector surface. To simulate a real detector f4:n –card is used for neutron particles, which tallies flux averaged over the detector cell volume. A tally multiplier card, fm4:n card specifies the material number (e.g. ^3He), and the reaction index {103 for (n, p) reaction of ^3He }. Fm-card calculates the quantity:

$$C \int \psi(E) R_m(E) dE$$

where, $\Psi(E)$ is energy dependent flux (particles/cm²) and $R_m(E)$ is an operator describing the reaction cross section (barns) of type-m. The constant C is atomic density (in atom per barn-cm). To obtain the true yields, this tally has to be multiplied by the detector cell volume. The energy range over which the integration is performed can be specified by a EN card.

3.1.7 Weight Windows

The weight window is a space-energy-dependent splitting and Russian roulette technique. For each space-energy phase space cell, the user supplies a lower weight bound. The upper weight bound is a user-specified multiple of the lower weight bound. These weight bounds define a window of acceptable weights. If a particle is below the lower weight bound, Russian roulette is played and the particle's weight is either increased to a value within the window or the particle is terminated. If a particle is above the upper weight bound, it is split so that all the split particles are within the window. No action is taken for particles within the window. Weight window provide an alternative means to

importances (IMP:n cards) for specifying space and energy importance functions. The advantages of weight windows are that they provide an importance function in space and time or space and energy; control particle weights; are more compatible with other variance reduction features such as the exponential transform (EXT:n card); can be applied at surface crossings, collisions, or both; the severity of splitting or Russian roulette can be controlled; can be turned off in selected space or energy regions; and can be automatically generated by the weight window generator. Weight windows can be either cell-based or mesh-based. A cell-based weight-window lower bound in a cell that is in a universe is interpreted as a multiplier of the weight-window lower bound of the filled cell.

3.1.8 Peripheral Cards

The number of histories, and description of the tally types to be printed etc., are specified at the end of the input deck by cutoff cards. The total history for each calculation is 10 million. The MCNP simulated calculations are run on the workstations with UNIX operation system: ULTRA 10. The running time is about one hour for each calculation.

3.2 Simulations with MCNP

The experiment was simulated by MCNP with standard samples of known neutron thermal absorption cross section values. The source, the sample and the detector are located in a water tank 97 cm in height. The source and sample were put as close as possible. The source-sample center distance was set 3.001 cm in MCNP input file. The sample has 3 cm in radius and 10.5 cm height. ^3He detector is treated as a cylinder

detector with a 0.5 cm in radius. Tittle and Crawford (1984) as well as Bussian (1991) stated that the detector orientation of 90° minimized the effect of sample scattering on the detector counts. Therefore the detector was oriented at 90° with respect to the source-sample center line for the initial calibration of the steady source experiment. The importance for each cell is specified in present experiment simulation while setting zero importance for the cell outside the water tank. In present steady source experiment simulation the antimony source is specified as a uniform source with the maximum energy 0.023 MeV. For result comparison between two sources, the ^{252}Cf source is also defined in MCNP input file specified with Watt fission spectrum. The calculation time for each sample is about one hour, during which 10 million histories were calculated for each. Perturbation effect is treated to reduce thermal effect. Weight window method is also used as variance reduction technique to control particle weight.

3.2.1 Calculation with Aqueous Samples

To encompass geologic aqueous solutions (borehole fluids) samples the known neutron thermal absorption cross section of standard aqueous samples range about from 22 CU to 75 CU was adequate. These aqueous samples were prepared by dissolving different amounts of pure sodium chloride in pure de-ionized water. Therefore the solutions of various concentrations as well as various absorption cross sections were gained. The theoretical cross sections of these standard samples were selected from MCNP nuclear and atomic data libraries. The primary sources of cross section data are evaluations from the Evaluated Nuclear Data File (ENDF) system.

The results from simulations of Both Antimony-Beryllium and Californium steady source experiments with sodium chloride solution samples are shown in Table 3-1, and the sensitivity comparison plots between two steady sources are shown in Figure 3-1. The counting rate data was normalized by divided by a normalization standard count rate. For these aqueous samples, sodium chloride solution with 1.0062 gm/cm^3 in density is chosen as the standard one for aqueous samples.

3.2.2 Calculation with Powder Samples

The experiment simulation was also calibrated with standard powder samples. To suitable for geologic rock powders samples, the known neutron thermal absorption cross section for samples range about from 2 CU to 20 CU was adequate. These powder samples were prepared by mixing pre-calculated amounts of silicon oxide and boric acid powder. Different amounts of silicon oxide and boric acid powder give various concentrations as well as various absorption cross sections powder samples. The theoretical cross sections of both silicon oxide and boric acid were pre-calculated by selected from MCNP nuclear and atomic data libraries. Therefore the theoretical macroscopic cross section of the mixture could be calculated from the Evaluated Nuclear Data File (ENDF) system.

The results from simulations of Both Antimony-Beryllium and Californium steady source experiments with silicon oxide and boric acid powder samples are shown in Table 3-2, and the sensitivity comparison plots between two steady sources are shown in Figure 3-2. The counting rate data was also normalized. For these powder samples, pure silicon oxide

powder sample with 1.678 gm/cm^3 in density was chosen as the standard one for powder samples.

	Sigma-A(CU)	Normalized-Cf	Normalized-Sb
Pure H ₂ O	22.060	1	1
0.87% NaCl	25.403	0.98632988	0.94495593
2.41% NaCl	31.076	0.95684096	0.88540484
5.12% NaCl	41.370	0.91392066	0.75923455
7.99% NaCl	52.703	0.86039738	0.67610836
10.13% NaCl	61.429	0.83803134	0.64836851
12.19% NaCl	70.077	0.81804231	0.61768979

Table 3-1 Data from simulations of Both Antimony-Beryllium and Californium steady source with sodium chloride solution samples

	Sigma-A(CU)	Normalized-Cf	Normalized-Sb
SiO ₂ (pure)	2.88	1	1
SiO ₂ + 0.3g H ₃ BO ₃	11.29	0.899197838	0.790388357
SiO ₂ + 0.5g H ₃ BO ₃	16.64	0.838402432	0.675333849
SiO ₂ + 0.8g H ₃ BO ₃	24.39	0.784598497	0.558600101
SiO ₂ + 0.9g H ₃ BO ₃	27.12	0.771831462	0.537889490

Table 3-2 Data from simulations of Both Antimony-Beryllium and Californium steady source with silicon oxide and boric acid powder samples

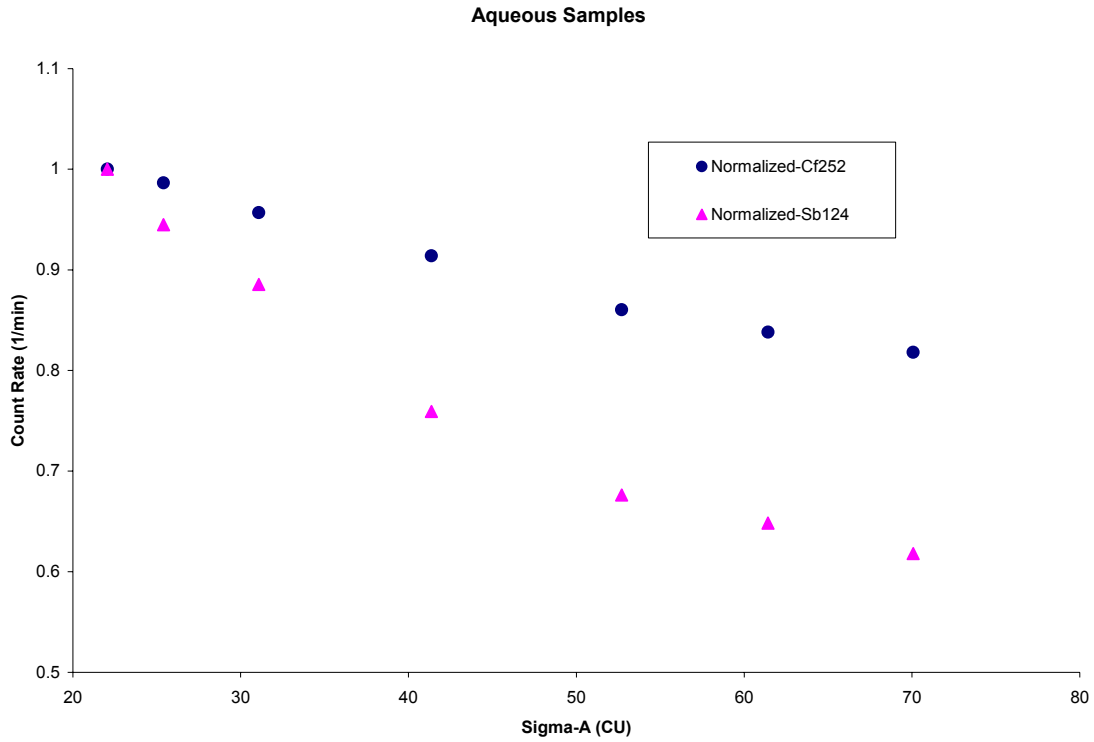


Figure 3-1. Sensitivity comparison from simulations of Both Antimony-Beryllium
and Californium steady source
with sodium chloride solution samples

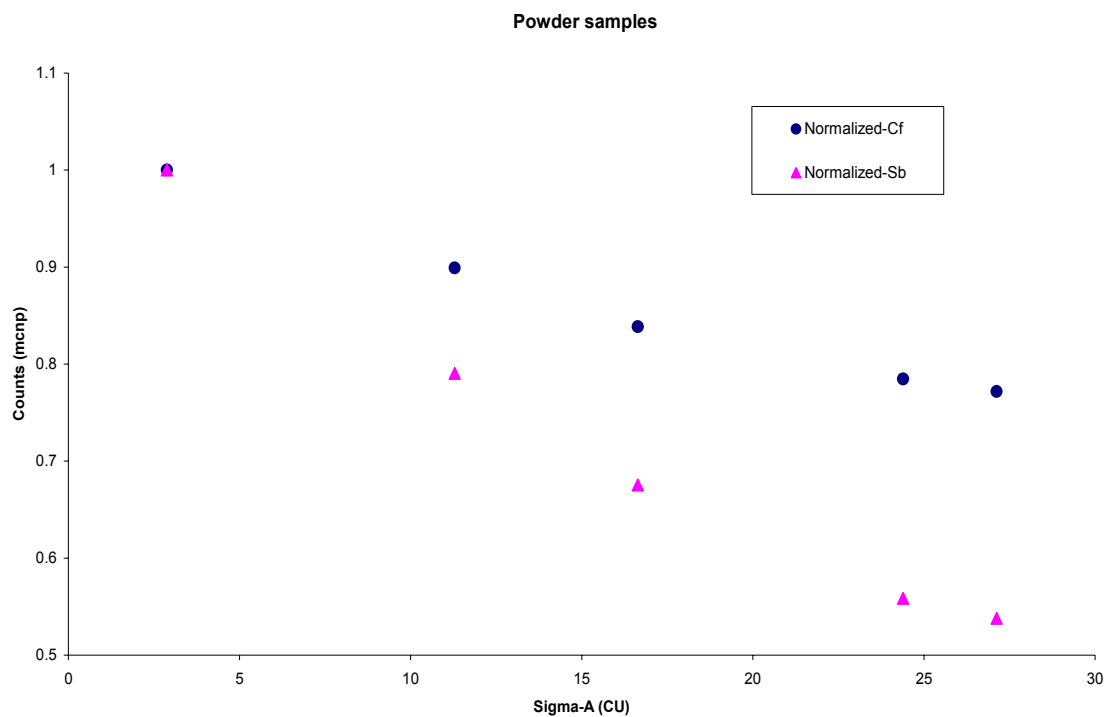


Figure 3-2. Sensitivity comparison from simulations of Both Antimony-Beryllium and Californium steady source with silicon oxide and boric acid powder samples

3.3 Discussions of Simulation

From Monte Carlo simulation calculations (Figure 3-1 and Figure 3-2) sensitivity gains improved with the ^{124}Sb -Be source compare to the ^{252}Cf source. The sensitivity improvement is expressed by the change of the slope of the linear function as absorption cross section versus counting rate. The comparison of the slopes and intercepts of the calibration curves between two sources is given in Table 3-3.

A steady source experiment was optimized and benchmarked by Monte Carlo simulation (MCNP code). An ^{124}Sb -Be source was introduced into the system which gives sensitivity improvement compare to Californium-252 source. However, such a source with very low energy (maximum energy is 23 Kev) would bring significant problem about thermal effect. Some treatments like perturbation effect ($S(\alpha,\beta)$) method has been used in MCNP simulation to reduce molecular binding effects. Thermal $S(\alpha,\beta)$ tables are not required, but they are absolutely essential to get correct answers in problems involving neutron thermalization. The data on these tables encompass those required for a complete representation of thermal neutron scattering by molecules and crystalline solids.

Sources	Results from simulation with Aqueous samples	Results from simulation with Powder samples
Californium 252	m : - 0.0039 (1/CU) (slope) C : 1.0813 (non-units) (intercept)	m : - 0.0094 (1/CU) (slope) C : 1.0136 (non-units) (intercept)
Antimony 124	m : - 0.0065 (1/CU) (slope) C : 1.1612 (non-units) (intercept)	m : - 0.0191 (1/CU) (slope) C : 1.0265 (non-units) (intercept)

Table 3-3 Sensitivity improvement--The comparison for slopes and intercepts of the calibration curves between two sources

Chapter 4

Experiments with ^{124}Sb -Be Source

Similar in principle to that described by Tittle and Crawford (1984) a steady source experiment device was developed. Plexiglass tubes used as waterproof holders for the source, sample and detector were made by a workshop at NC State. Both aqueous samples and powder samples were used in the experiments to encompass geological samples. A ^3He was used as thermal neutron detection medium. The ^{124}Sb -Be source was obtained from Frontier Technologies source company and also encapsulated at NC State prior to activated in the NC State PULSTAR Reactor. A ^{252}Cf source used in previous work by Tallavarjula and Sood was used for sensitivity improvement comparison.

4.1 Experiment System

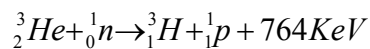
The side view of the new experiment design is shown in Figure 4-1. The system consists of a moderating tank of 106.68 cm in diameter and filled with water up to 99.5 cm in height. Plexiglass tubes, which are used in the present design because of their good properties under radiation, are designed specially as the holders for the source, the sample and the detector so that these can be waterproof during the experiments and the detector can be held grazing the sample container surface.

A cylindrical polyethylene bottle with 6 cm in diameter and 10.5 cm in height was chosen to contain the aqueous or powder samples. From the conclusion of Tallavarjula^[5]'s research, a sample volume in the range (250 cm³ to 300 cm³) should give reasonable

sensitivity. In present experiment the volume of the sample is determined as 275 cm³. A string is designed to move the samples during the experiment for various cross section measurement points.

A ¹²⁴Sb-Be neutron source was welded into an plastic encapsulation and activated in the PULSTAR reactor before experiments. It was placed with its axis along the axis of the moderating tank with its center about 45 cm below the center of the tank. The source encapsulation external dimensions are 2.1 cm in diameter and 15 cm in length. It is held very close to the sample, with a distance of about 5 cm from the source axis to the sample axis. The steady neutron energy spectrum is uniform with 23 KeV in maximum approximately. A string is used to move the source before and after the experiment.

The ³He detector is widely used as detection tools for thermal neutrons. The reaction is expressed by,



The cross section for the reaction is large so that the counting efficiency of the detector can be high enough with small active dimensions. The thermal neutron cross section for this reaction is 5330 barns at 2200 m/s and falls off with 1/v energy dependence. The orientation of the angle used in experiment is 90° and 180° (Figure 2-2).

4.2 Counting Rate Electronics

The counting rate electronic circuit is used to measure the counting rate of the pulse from the ^3He detector. The pulse out of the detector goes through a preamplifier. After that, they are processed by a linear amplifier. The linear amplifier provides voltage gain to the preamplifier pulses, so that the pulses can be counted easily. The amplified linear pulses are converted to logic pulses by a single channel analyzer (SCA). When set in the integral discriminator mode, SCA produces a logic pulse only if the linear input pulse exceeds a set discrimination level. If the input pulse is below the lower level discriminator (LLD), no output appears. The numbers of logic pulses are recorded by a scaler. They are also accumulated over a certain period of time set for each measurement. The modules of the measure system are shown in Figure 4-2.

The parameters of experimental apparatuses were preset by,

$$\text{Gain (AMP)} = 100 \times 1.5 \quad \text{Lower (SCA)} = 0.3 \text{ V}$$

The high voltage plateau determination test was done to determine the operating voltage. The test was begin at 550 V and was raised by small increment each time. A one-minute count was set. The plateau curve is shown in Figure 4-3. From the test results, the operating voltage is chosen at 1400 V.

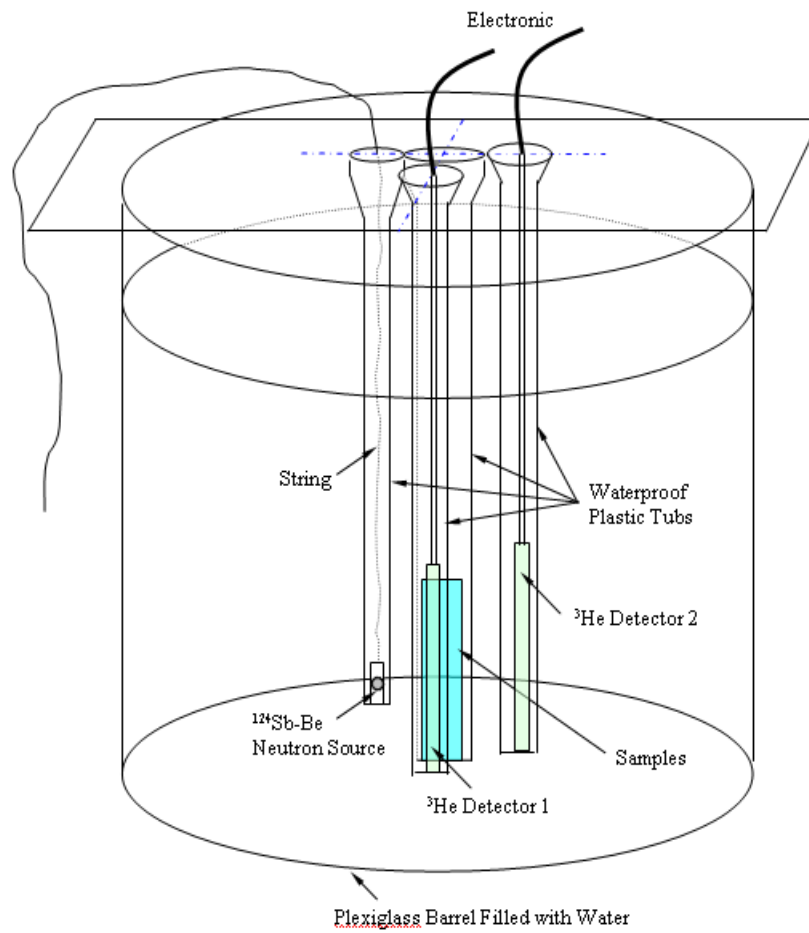


Figure 4-1. Side view of the experiment device

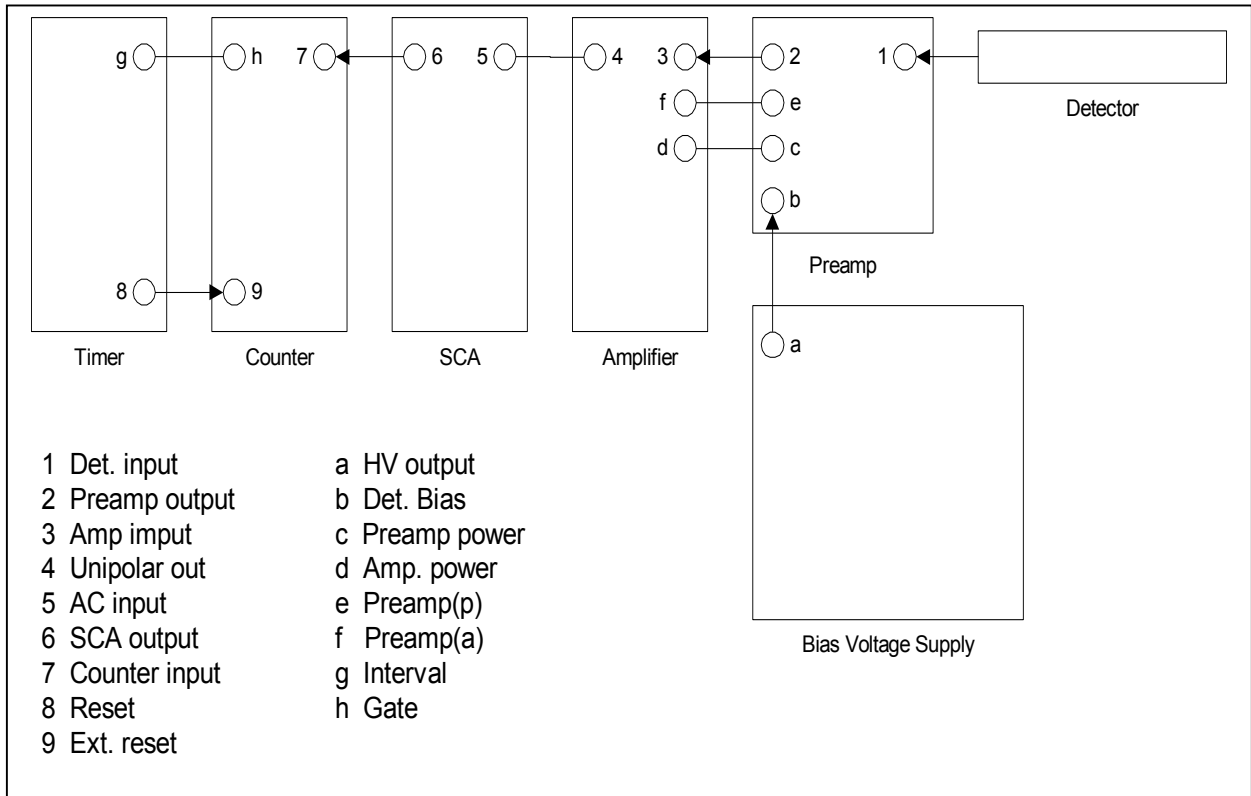


Figure 4-2. The electronic circuit system for cross section measurement

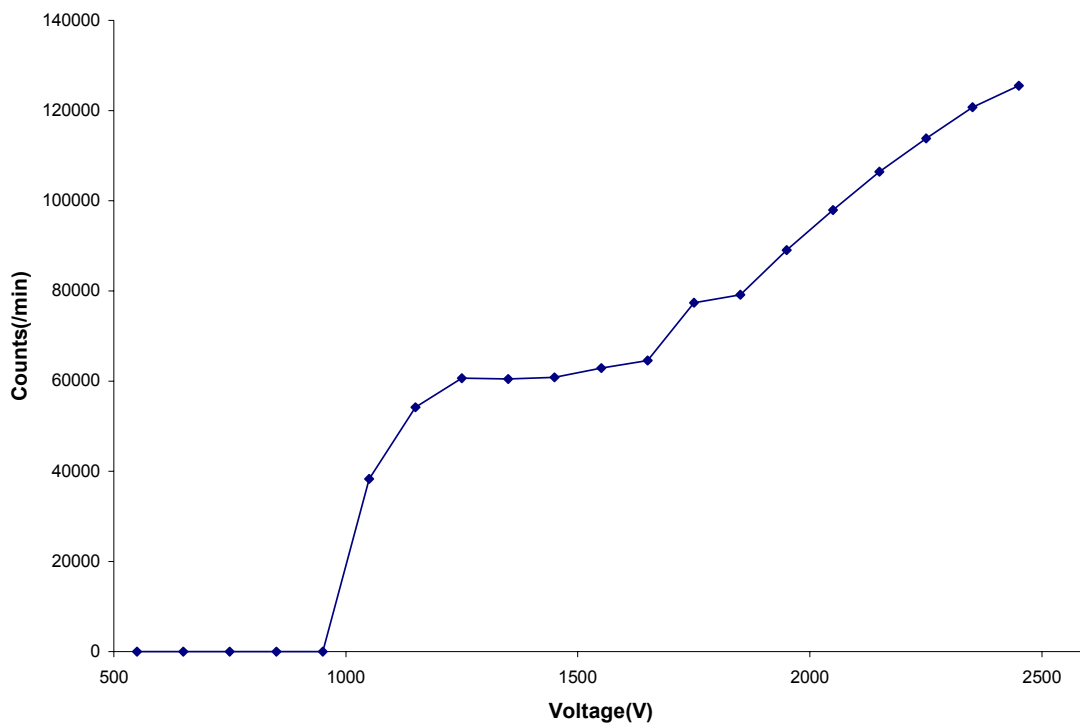


Figure 4-3. The operating high voltage plateau determination

4.3 Preparation for Samples

The experiment was calibrated with standard samples of known neutron thermal absorption cross section values. To encompass geologic samples the cross section range of 2 CU to 20 CU was adequate for powder samples while the cross section range from 22 CU to 75 CU was adequate for aqueous samples. In present experiments, the mixture of pure silicon oxide and boric acid powder were chosen as powder samples as well as Sodium chloride solutions were chosen as aqueous samples. In addition, pure sodium carbonate powder samples and pure sodium sulfate powder samples were also used as calibration standards. The theoretical macroscopic cross sections of these standards can be calculated from the microscopic cross section values of these elements at 2200 m/s and the sample density. The thermal neutron microscopic cross sections (2200 m/s) for pure element used in experiment as standard aqueous and powder samples are listed in Table 4-1.

4.3.1 Aqueous Samples

The standard aqueous samples were prepared by dissolving different amounts of pure sodium chloride in pure de-ionized water. Therefore solutions providing various macroscopic absorption cross sections were obtained. The amounts of sodium chloride compound were pre-calculated, and the densities of solutions were pre-known, therefore the solution weight and density can be calculated as formula given below,

$$W_{\text{solution}} = W_{\text{NaCl}} + W_{\text{H}_2\text{O}} \quad \text{Total solution weight}$$

$$V_{\text{solution}} = W_{\text{NaCl}}/\rho_{\text{NaCl}} + W_{\text{H}_2\text{O}}/\rho_{\text{H}_2\text{O}} \quad \text{Total solution volume}$$

$$\rho_{\text{solution}} = W_{\text{solution}} / V_{\text{solution}} \quad \text{Solution density}$$

W_{NaCl} and ρ_{NaCl} represent the weight and the density of compound sodium chloride. $W_{\text{H}_2\text{O}}$ and $\rho_{\text{H}_2\text{O}}$ represent the weight and the density of water. The weight of each element in sodium chloride is given by,

$$W_{\text{Na}} = (W_{\text{NaCl}} / M_{\text{NaCl}}) \times A_{\text{Na}} \quad \text{Weight of Sodium}$$

$$W_{\text{Cl}} = (W_{\text{NaCl}} / M_{\text{NaCl}}) \times A_{\text{Cl}} \quad \text{Weight of Chlorine}$$

$$W_{\text{H}} = (W_{\text{H}_2\text{O}} / M_{\text{H}_2\text{O}}) \times A_{\text{H}} \quad \text{Weight of Hydrogen}$$

$$W_{\text{O}} = (W_{\text{H}_2\text{O}} / M_{\text{H}_2\text{O}}) \times A_{\text{O}} \quad \text{Weight of Oxygen}$$

$M_{\text{H}_2\text{O}}$ and M_{NaCl} represent the molecule numbers of water and sodium chloride. Then the theoretical macroscopic cross section of the aqueous samples could be calculated by,

$$\Sigma = \rho \times N_A \times \sum_i^I (w_i / A_i) \times \sigma_i$$

Where N_A is the Avogadro's constant. σ_i is the microscopic cross section of the element i . A_i is the atomic mass of the element i . Capital I represents the total number of elements in the mixture. The pre-calculated macroscopic cross sections of standard aqueous samples were listed in Table 4-2.

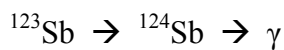
4.3.2 Powder Samples

The experiment was also calibrated with standard powder samples. ^{10}B has very high thermal neutron absorption cross sections. Thus boric acid was introduced to make powder standards. Powder samples used in the experiments were prepared by mixing pure silicon oxide and boric acid powders. To represent geologic rock powders samples, the known neutron thermal absorption cross section of standard samples range was

chosen from 2 CU to 20 CU. The amounts of compounds silicon oxide and boric acid were pre-calculated, and their densities and weights were known, and the theoretical macroscopic cross section of the mixture powder samples was calculated. The formula used for element weight and powder sample macroscopic cross sections calculations were similar to those used for aqueous samples. However because element Oxygen was appeared in both silicon oxide and boric acid, the weights of Oxygen were added together. Pure sodium carbonate powder samples and pure sodium sulfate powder samples were also used as calibration standards. The pre-calculated macroscopic cross sections of standard aqueous samples are listed in Table 4-3.

4.4 Preparation for Source

A ^{124}Sb -Be neutron source was encapsulated by a workshop at NC State. After encapsulation, the source has an external dimension of 2.1 cm diameter and 15 cm length. A string was designed on the top for moving source before and after experiments. The source should be activated in the reactor for about 15 hours and be shut down for about 17 hours before used in experiments. The estimate output is 4000 neutron/sec. Actions occurred inside the source pellet to give out neutrons by,



The source was placed with its axis along the axis of the moderating tank during the experiment, but its center is about 45 cm below the center of the tank. The procedure of encapsulation and testing of ^{124}Sb -Be source are given in appendix D and appendix E. The calculation for source pallet mass and activation time are given in appendix F.

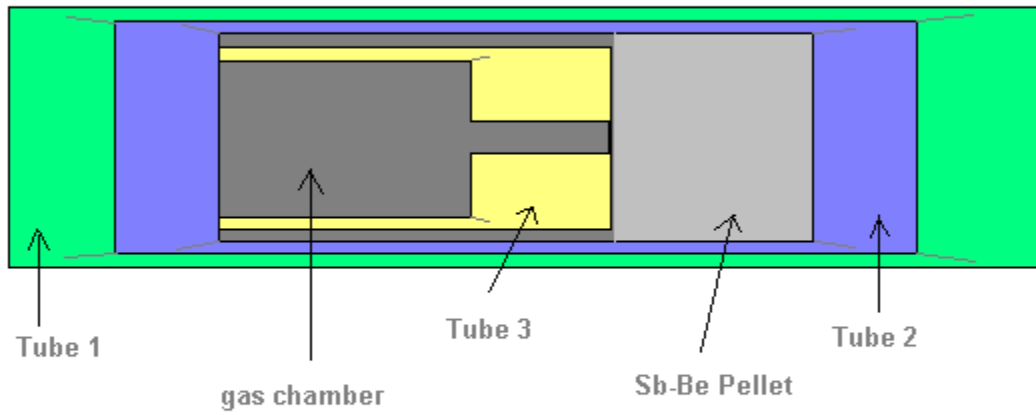


Figure 4-4. The structure of the source encapsulation

Element	Z	A	σ_a (barns)
H	1	1.008	0.3326
B	5	10.820	758.4
C	6	12.001	0.0037
N	7	14.008	1.880
O	8	15.999	0.0002
Na	11	22.991	0.531
Si	14	28.086	0.171
S	16	32.064	0.520
Cl	17	35.457	33.800
K	19	39.098	2.100
Ca	20	40.080	0.430

Table 4-1. The thermal neutron microscopic cross sections (2200 m/s) for pure element as standard aqueous and powder samples

Sodium Chloride Solutions	Solution Density $\rho_{\text{solution}} (\text{gm/cm}^3)$	Σ_a (CU)
Pure H ₂ O	1.0000	22.242
0.87 % NaCl	1.0062	25.403
2.41 % NaCl	1.0172	31.076
5.12 % NaCl	1.0367	41.408
7.99 % NaCl	1.0577	52.703
10.13 % NaCl	1.0736	61.429
12.19 % NaCl	1.0890	70.077

Table 4-2. The pre-calculated macroscopic cross sections of standard aqueous samples

Mixture Powder	Solution Density	Σ_a
Solutions	$\rho_{\text{solution}} \text{ (gm/cm}^3\text{)}$	(CU)
Pure SiO ₂	1.678	2.88
SiO ₂ + 0.31g H ₃ BO ₃	1.678	11.29
SiO ₂ + 0.52g H ₃ BO ₃	1.678	16.64
SiO ₂ + 0.82g H ₃ BO ₃	1.678	24.39
SiO ₂ + 0.91g H ₃ BO ₃	1.678	27.12

Table 4-3. The pre-calculated macroscopic cross sections of standard powder samples

4.5 Calibration with Standard Samples

4.5.1 Experiments with ^{252}Cf and $^{124}\text{Sb-Be}$ Source in new apparatus

The calibration experiments were done with both $^{124}\text{Sb-Be}$ and ^{252}Cf steady sources and both aqueous and powder samples. The counting rates were normalized by being divided by a normalization standard counting rate. For aqueous samples a water sample was chosen as the standard, while for powder samples, a pure silicon oxide powder sample with 1.678 gm/cm^3 in density was chosen. A ^{252}Cf source (3.5 μg as of 03/31/1993, Model SR-CF-100) with 7.3×10^6 n/s neutron output and a $^{124}\text{Sb-Be}$ source (^{124}Sb 10mCi/ ^{122}Sb 16mCi of 05/23/02) with 4.0×10^3 n/s neutron output were used for measurement comparison. The detector was located in 90° and 180° orientations separately and 5 minutes counting rates were used for each measurement. The sample was removed and reintroduced into the system, recording the counting rate five times. The mean counting rates were obtained by averages and were normalized to form standard one. Calibration curves of neutron absorption cross-sections measurements with both $^{124}\text{Sb-Be}$ and ^{252}Cf sources are shown in Figure 4-5 and Figure 4-6.

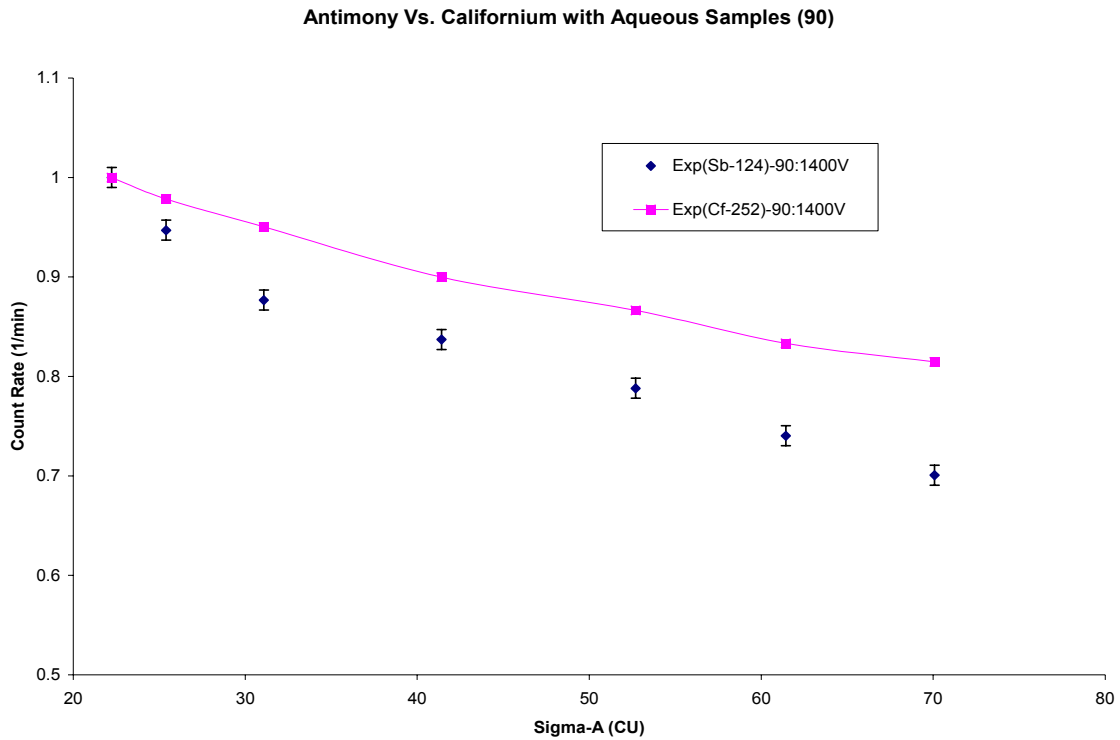


Figure 4-5. Sensitivity improvement comparison from experiment measurements for absorption cross section between two sources with aqueous samples (90°)

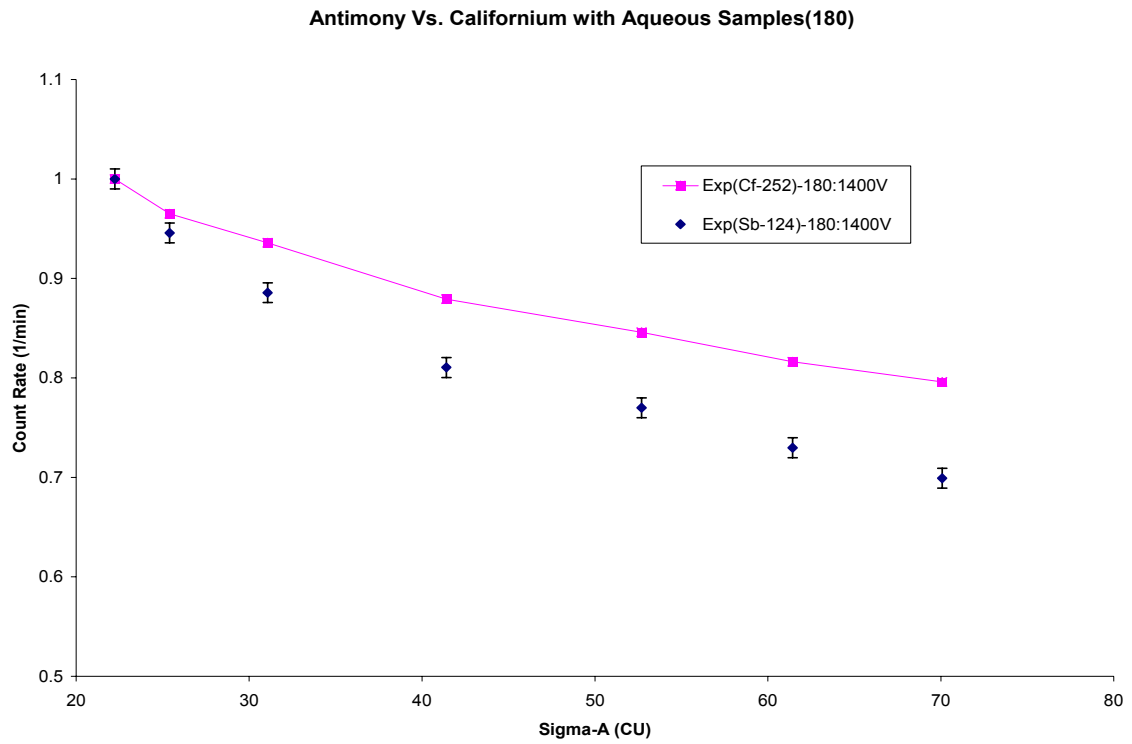


Figure 4-6. Sensitivity improvement comparison from experiment measurements for absorption cross section between two sources with aqueous samples (180°)

4.5.2 Semi-empirical model

A semi-empirical model was proposed to describe both absorption and scattering cross-sections of the discrete aqueous and powder samples in Tallavarjula^[5]'s work. Two detector locations (90° and 180° orientations) are introduced for measurements. The detector response is modeled by an exponential attenuation term given by,

$$R(\theta) = A(\theta)\exp[-d(\theta)\Sigma_{eff}]$$

Where $R(\theta)$ is the detector yield at the orientation θ . $A(\theta)$, $d(\theta)$ and $k(\theta)$ are empirical parameters and can be determined using a least squares method on the cross-sections values of the known standards. Σ_{eff} is the effective cross-sections defined by taking into account both the absorption and the scattering cross-sections of the sample as:

$$\Sigma_{eff} = \Sigma_a + k(\theta)\Sigma_s$$

A similar, new semi-empirical model is introduced in Sood^[6]'s work. The method of two detector locations used to describe both absorption and scattering cross-sections are same as the old model. However, the improvement is that new model allows independent behavior of the thermal neutron absorption and scattering cross-sections. The response function of the detector is given by

$$R(\theta) = c(\theta)\exp[-a(\theta)\Sigma_a - b(\theta)\Sigma_s]$$

If calibration measurements are made at 90° and 180° orientations, two simultaneous equations will resolve Σ_a and Σ_s explicitly. Figure 4-7 shows the absorption cross-sections measurement results from source ¹²⁴Sb-Be and ²⁵²Cf with the aqueous samples for 90° and 180° detector locations by MCNP simulations according to semi-empirical model. Figure 4-8 gives the comparison results between MCNP simulations and

experimental measurements. After normalization the simulation results fit the experimental curve very well. The detector responses of simulation and experiments at both 90° and 180° orientations are also shown in Figure 4-9 and Figure 4-10. Sensitivity improvement was expressed by the change of the slope of the linear function as absorption cross-sections versus counting rates. The comparison for slopes and intercepts of the calibration curves between two sources for both simulated calculation and experimental measurements is given in Table 4-5.

4.5.3 Compare to previous work (²⁵²Cf Source in paraffin box)

For the reason of comparing sensitivity improvements, the experiments with ²⁵²Cf source in paraffin box were done for aqueous samples only. The calibration curve is shown in Figure 4-11. And the experiment data compare to Sood^[6]'s results are listed in Table 4-4. The counting rates were normalized. The slope is closed to the previous value and the errors of slope and intercept are acceptable.

	Repeat Experiment Result	Sood's Result
Slope (1/CU)	-0.0034	-0.00336
Error of Slope (1/CU)	5.83e-05	4.77e-05
Intercept (non-units)	1.0387	1.0572
Error of Intercept (non-units)	1.019e-03	2.59e-03

Table 4-4. Repeated experiments data versus Sood's results

The results showed in 4.5.1 and 4.5.2 are all experiments done in water tank apparatus. To present the sensitivity improvement from previous work, the comparison between those done in paraffin box with ^{252}Cf source and those done in water tank with ^{124}Sb -Be source is given in Figure 4-12. The results seem not being improved too much from Sood^[6]'s experiments. Because the scattering effects from moderating medium are significant in these measurements, this cannot be ignored in data analysis and conclusions. A Cadmium shield is considering to reduce neutron scattering effect in the later experiments.

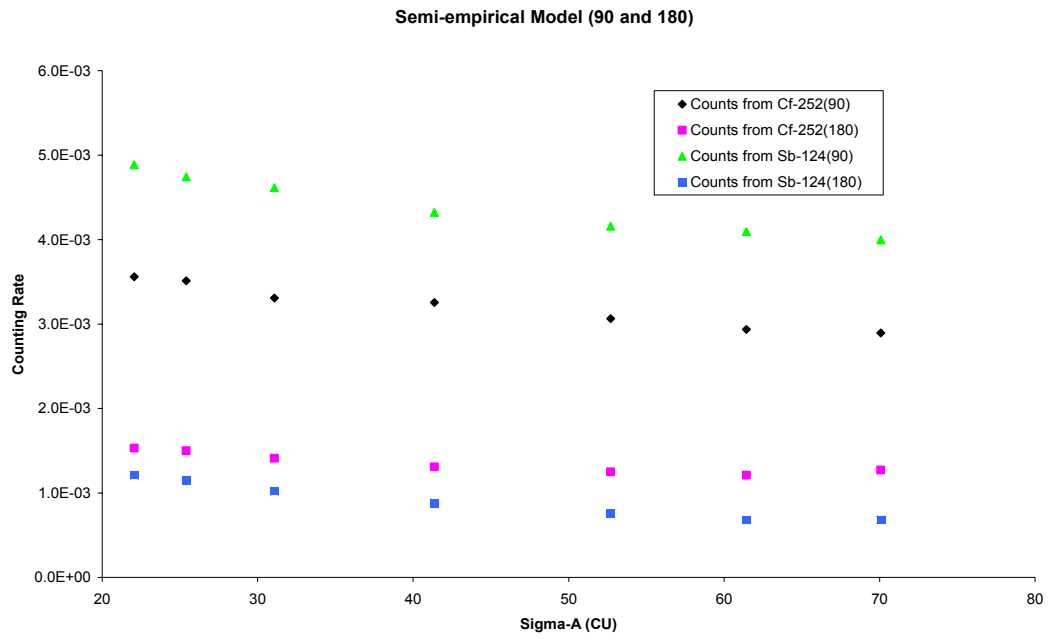


Figure 4-7. Semi-empirical Model of Absorption cross section measurement for both 90° and 180° detector locations by MCNP simulations

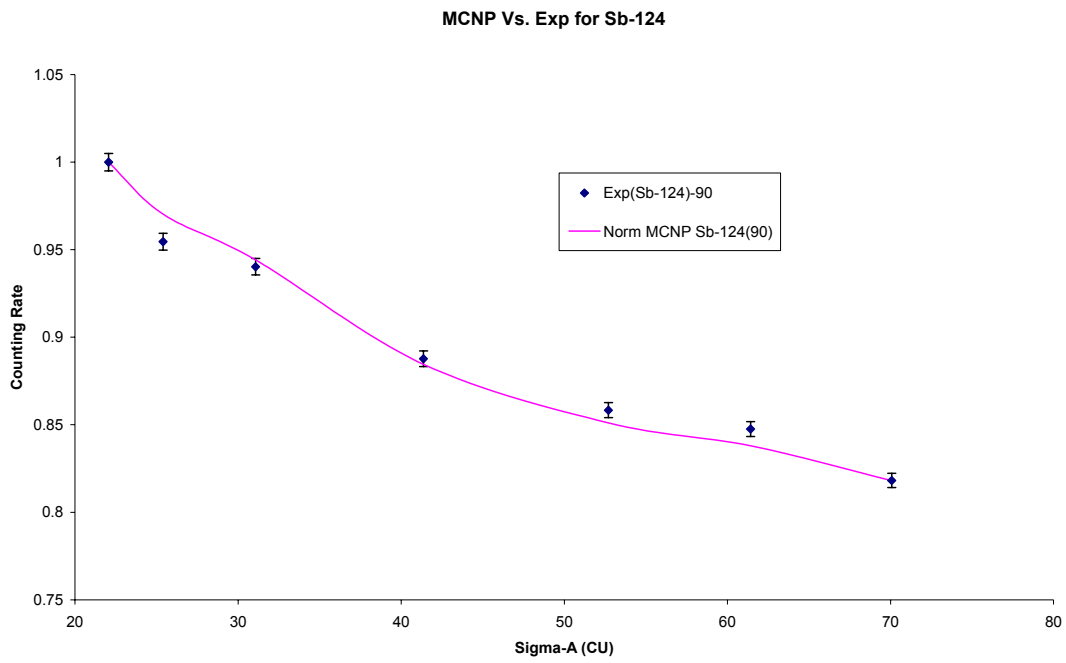


Figure 4-8. Comparison between MCNP simulation and experimental measurements with ^{124}Sb -Be source

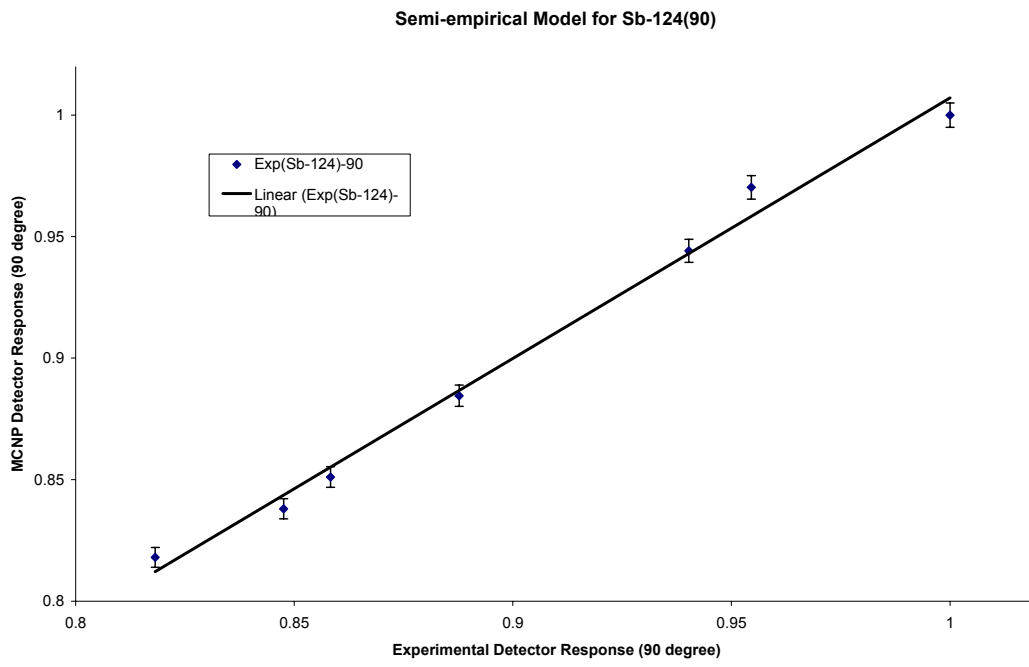


Figure 4-9. Detector response with Semi empirical Model (90°)

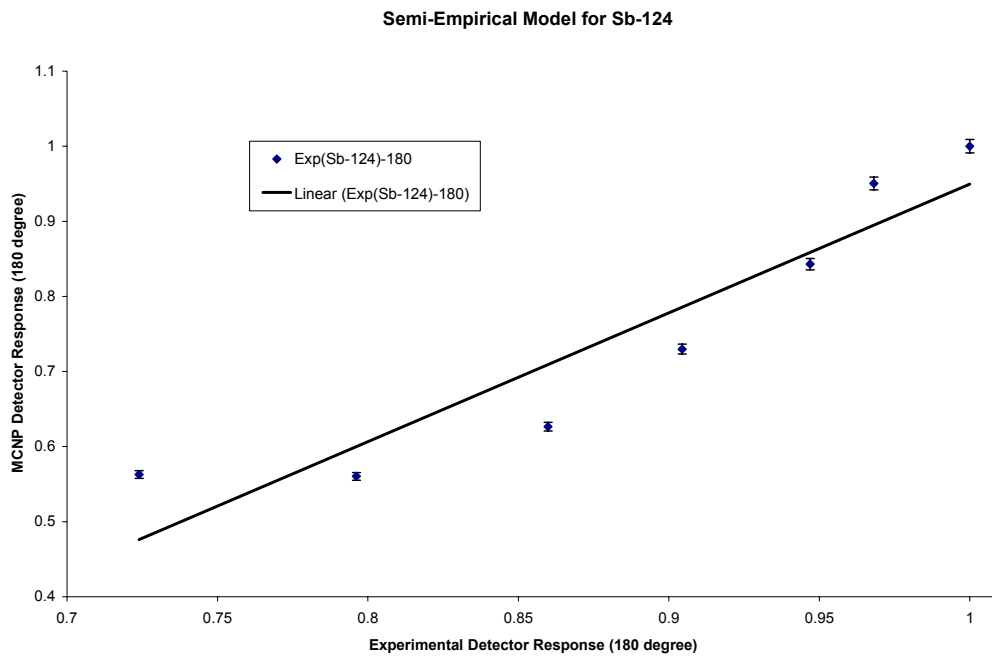


Figure 4-10. Detector response with Semi empirical Model (180°)

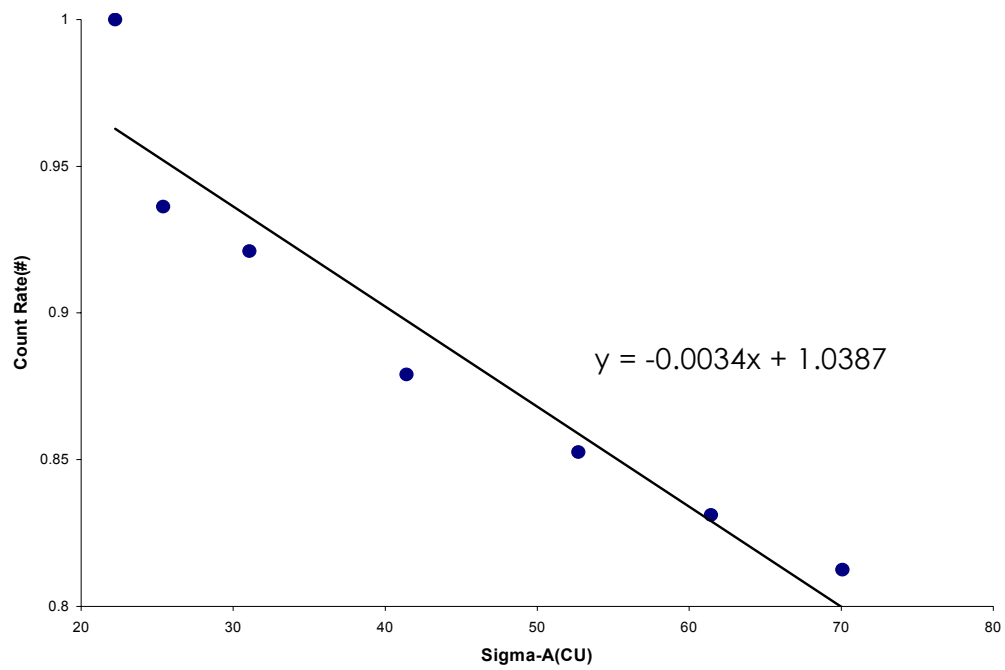


Figure 4-11. Calibration Curve of Repeat Experiments with ^{252}Cf Source and paraffin box

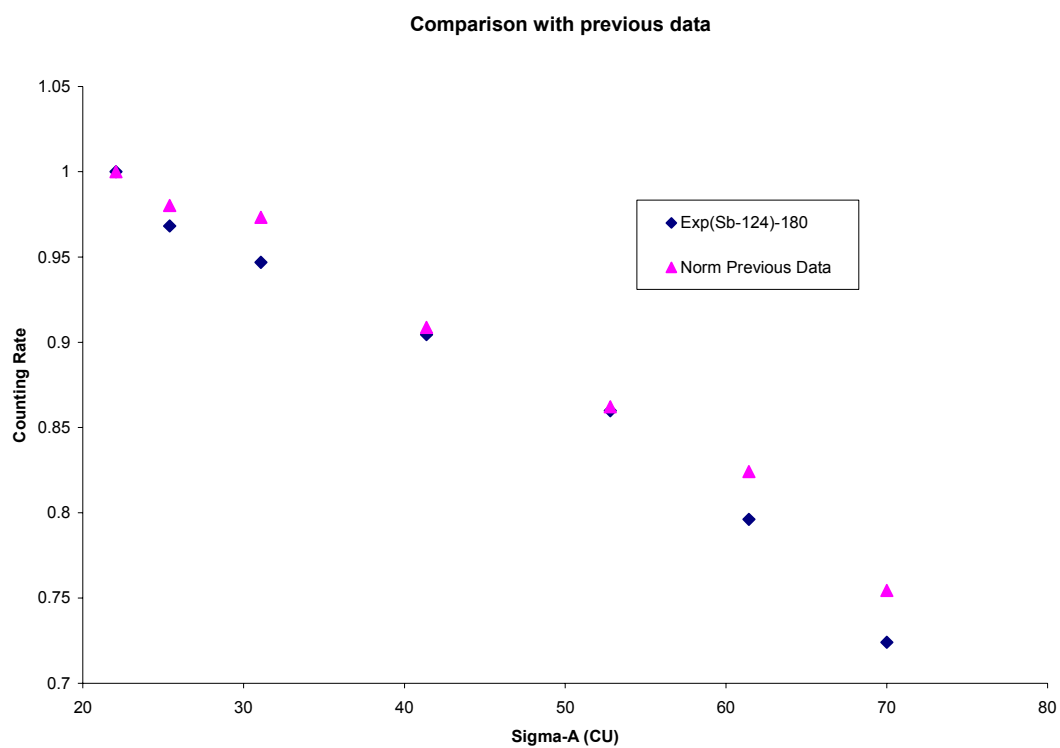


Figure 4-12. Comparison between results of Antimony source in water tank and Californium source in paraffin box

4.6 Discussion for Experiment Measurements

An improved apparatus and a $^{124}\text{Sb-Be}$ source were benchmarked by Monte Carlo simulation then was introduced into the experimental system for both aqueous and powder samples measurements. Such a source would bring some problems about gamma rays. The adjustments for the lower level of SCA should reduce gamma rays effect to minimum. The half life time of $^{124}\text{Sb-Be}$ is very short, only about 2.5 days. Therefore the counting rates will diminish quickly day by day. The results normalization will keep multiple measurements to an agreement. Sensitivity improvement was expressed by the change of the slope of the linear function as absorption cross-sections versus counting rates. From Table 4-5, the lower energy source ($^{124}\text{Sb-Be}$) offered better sensitivity improvement.

A semi-empirical model was successfully applied to verify both absorption and scattering cross-sections. The simulation data and experimental results are fitted very well. However, the thermal effect still has some problems to the simulation results. More improvements should be considered about gamma rays during the later experiments.

Sources	Results from MCNP simulation	Results from experiment
	with Aqueous samples	with Aqueous samples
^{252}Cf	m : - 0.0039 (1/CU) (slope) C : 1.0813 (non-units) (intercept)	m : - 0.0039 (1/CU) (slope) C : 1.0746 (non-units) (intercept)
$^{124}\text{Sb-Be}$	m : - 0.0065 (1/CU) (slope) C : 1.1612 (non-units) (intercept)	m : - 0.0059 (1/CU) (slope) C : 1.0895 (non-units) (intercept)

Table 4-5. Sensitivity improvement with $^{124}\text{Sb-Be}$ source
compare to ^{252}Cf source

Chapter 5

Conclusions and Future Work

5.1 Summary and Conclusions

1. A steady source experiment technique for neutron absorption cross-sections measurement was optimized and benchmarked by Monte Carlo simulation (MCNP code). An Antimony-124 (Sb) source was introduced into the system with lower energy 23 KeV. From both simulated calculations and the experimental results, the sensitivity for absorption cross section measurement with ^{124}Sb -Be source has been improved compare to ^{252}Cf source has done.
2. Such a very low energy (maximum energy is 23 Kev) source would bring significant problem about thermal effect. Some treatments like perturbation correction ($S(\alpha,\beta)$) method and weight window method has been used in MCNP simulation to reduce the molecular binding effect.
3. Monte Carlo studies were also used for some attenuation tests with both aqueous samples and powder samples at the beginning, so that the behavior of thermal neutron flux perturbation in the vicinity of a sample could be demonstrated. The thermal neutron flux can be described as an exponential function of the positions.
4. Using the knowledge obtained from MCNP simulations, the experimental apparatus construction and the source shielding would be relatively accurate. Experimental responses and MCNP responses matched very well for Cf-252 source. However, for Sb-124 Source, Experimental responses still have less slope than simulation. In MCNP calculation, we make some ideal assumptions. So the results would be obtained under

an ideal situation. During experiments, Antimony source with short half-life shows a big instability, which affects the response very much. The density of the sample is also not exactly same as calculated by standard formula. These factors will make less sensitivity than simulations.

5. During the experiments the gamma rays brought big trouble on counting rates stability. The lower level of SCA was adjusted carefully and worked together with MCA to reduce the gamma rays effect to minimum.
6. Neutron scattering in moderator will affect the detector's counting rates slightly. This kind of effect is minimized on 90° orientation. The detector response on 90° orientation was given a little better results then the one on 180° orientation.
7. A semi-empirical model was successfully developed and applied to incorporate both absorption and scattering cross-sections in MCNP simulated calculations. This model was then confirmed and validated in experimental measurements.
8. Compared to the previous work, the results seem not being improved too much from Sood's experiments. Because the scattering effects from moderating medium cannot be ignored in data analysis and conclusions.

5.2 Future Work

1. Gamma rays shielding is still a problem. More improvement should be considered during the later work.
2. A Cadmium (Cd) shield around the detector is being considered to reduce the scattering effect in the later experiments.

3. Experiments for geologic rock samples will be done after calibrations, which will be more helpful to the applications in the oil well logging industries. The absorption cross sections gained from experiment results would compare to those from Monte Carlo simulations.

Reference

- [1] Tittle, C.W., Crawford, G.W., 1983. Measuring the thermal neutron absorption cross section of rocks. Log analy.
- [2] Salaita, G.N., 1985. A system for measuring thermal neutron absorption cross section of small liquid and rock samples. SPWLA 26th Annual Logging Symposium Transactions, Paper Q.
- [3] Mickael, M.w., 1988. Monte Carlo simulation of dual-spaced neutron porosity well logging tool responses. Ph.D. Thesis NCSU.
- [4] Bussia, A.E., Jetter, W.A., Supernaw, I.R., 1991. A method for measuring thermal neutron absorption and transport cross sections. Nucl. Geo 5(4), 439-449
- [5] Tallavarjula, S., 1995. Thermal neutron cross section measurement for geological materials. Ph.D. Thesis, NCSU.
- [6] Sood, A., Gardner, R.P., Gray, T.K., 2000. Steady neutron source measurement method for Σ_a and Σ_s in geological samples. Applied Radiation and Isotopes, 53, 603-616.
- [7] Knoll, G.F., 1989. Radiation Detection and Measurement. John Wiley & Sons, New York.
- [8] Beckurts, K.H., Wirtz, K., 1964. Neutron Physics. Springer-Verlag, New York.
- [9] Mughabghab, S.F., divadeenam, M., Holden, N.E., 1981. Neutron Cross Sections, Vol. Part A. Academic Press, New York.

- [10] MCNP- a general purpose Monte Carlo n-particle transport code version 4C. LA-7396-M, Los Alamos National Laboratory.
- [11] Weast, R.C., 1983. CRC Handbook of Chemistry and Physics. The Log Analyst.
- [12] **Frontier Technology Company**, 1985. Antimony Source Manual.


```

c
c m2  1001.50c  -0.1119013  8016.50c  -0.8880987  $ water sample
c
m2  1001.50c  -0.09757
    8016.50c  -0.78053
    11023.51c -0.04795
    17000.51c -0.07395
                                           $ NaCl + H2O AWL5 rho=1.089
c
c m2  1001.50c  -0.09986
c     8016.50c  -0.79884
c     11023.51c -0.03985
c     17000.51c -0.06145
                                           $ NaCl + H2O AWL4
rho=1.0736
c
c m2  1001.50c  -0.10223
c     8016.50c  -0.81787
c     11023.51c -0.03143
c     17000.51c -0.04847
                                           $ NaCl + H2O AWL3
rho=1.0577
c
c m2  1001.50c  -0.10542
c     8016.50c  -0.84338
c     11023.51c -0.02014
c     17000.51c -0.03106
                                           $ NaCl + H2O AWL2
rho=1.0367
c
c m2  1001.50c  -0.10843
c     8016.50c  -0.86747
c     11023.51c -0.00948
c     17000.51c -0.01462
                                           $ NaCl + H2O AWL1
rho=1.0172
c
c m2  1001.50c  -0.11014
c     8016.50c  -0.88116
c     11023.51c -0.00342
c     17000.51c -0.00528
                                           $ NaCl + H2O AWL1/2
rho=1.0062
c
c m2  14000.51c -0.4666667
c     8016.50c  -0.5333333
                                           $ SiO2
c
c m2  1001.50c  -1.0e-8
c     5010.50c  -1.0e-8
c     5011.35c  -1.0e-8
c     8016.50c  -0.5325
                                           $ SiO2 + 0.0 gm H3BO4
c
c m2  1001.50c  -0.00003039
c     5010.50c  -0.00001922
c     5011.35c  -0.00008951
c     8016.50c  -0.53260669
c     14000.51c -0.46725418
                                           $ SiO2 + 0.3 gm H3BO4
c
c m2  1001.50c  -0.5161e-4
c     5010.50c  -0.3264e-4
c     5011.35c  -0.152e-3
c     8016.50c  -0.5327124

```

```

c      14000.51c -0.4670514          $ SiO2 + 0.5 gm H3BO4
c
c m2   1001.50c -0.8392104e-4
c      5010.50c -0.5217312e-4
c      5011.35c -0.2478778e-3
c      8016.50c -0.5329832
c      14000.51c -0.4666328          $ SiO2 + 0.8 gm H3BO4
c
c m2   1001.50c -0.00008930
c      5010.50c -0.00005648
c      5011.35c -0.00026303
c      8016.50c -0.53290021
c      14000.51c -0.46669102          $ SiO2 + 0.9 gm H3BO4
c
c m2   11023.51c -0.3931624
c      17000.51c -0.6068376          $ NaCl (pure)
c
c m2   11023.51c -0.4339623
c      8016.50c -0.4528302
c      6012.50c -0.1132075          $ Na2CO3 (pure)
c
c m2   11023.51c -0.3239437
c      8016.50c -0.4507042
c      16032.51c -0.2253521          $ Na2SO4 (pure)
c
c m2   20000.51c -0.3973600
c      8016.50c -0.4755948
c      6012.50c -0.1189800          $ CaCO3 (pure)
c
c m2   20000.51c -0.2980200
c      8016.50c -0.5787208
c      6012.50c -0.0892350
c      1001.50c -0.0279753          $ CaCO3 + 0.9 H2O
c
c m2   20000.51c -0.2980200
c      8016.50c -0.5787208
c      6012.50c -0.0892350
c      1001.50c -0.0279753          $ CaCO3 + 0.8 H2O
c
c m2   20000.51c -0.2980200
c      8016.50c -0.5787208
c      6012.50c -0.0892350
c      1001.50c -0.0279753          $ CaCO3 + 0.7 H2O
c
c m2   20000.51c -0.2980200
c      8016.50c -0.5787208
c      6012.50c -0.0892350
c      1001.50c -0.0279753          $ CaCO3 + 0.6 H2O
c
m3    2003.50c -1.0                  $ He-3
c
c      importance cards
c
imp:n 1 7r 0
c
c      Weight Window Generation cards
c

```

```

c   tally src-cell x det. center co-ordinates flag
c wwg      14      4      0    11.5    0    0    0
wwg      24      4      0    5.001    6.5    0    0
wwge:n    2.0e-6    1.0e-1    10
c
c   source specification cards
c
sdef erg=d1 wgt=1 pos=0 0 0
sil 0 0.023
spl 0 1                                $ Uniformed Antimony source
Max=23KeV
c
c sc1 Cf-252 Watt spectrum
c spl -3 1.025 2.926                    $ Californium source
c
c   tally specification cards
c
c f14:n    2
c fm14     -1 3 103
f24:n     3
fm24     -1 3 103
c
c   problem cutoff cards
c
c cut:n j 0.01
prdmp 25000 5000
c nps 1000000
nps 1000
print 110

```

APPENDIX B

Style and model of electronic apparatuses

Detector:	^3He
Bias Voltage Supply:	ORTEC 456
Pre-Amplifier:	ORTEC 109 PC
Amplifier:	ORTEC 575
Single Channel Analyzer:	TENNELEC TC 450
Counter:	TENNELEC TC 531
Timer:	TENNELEC TC 541

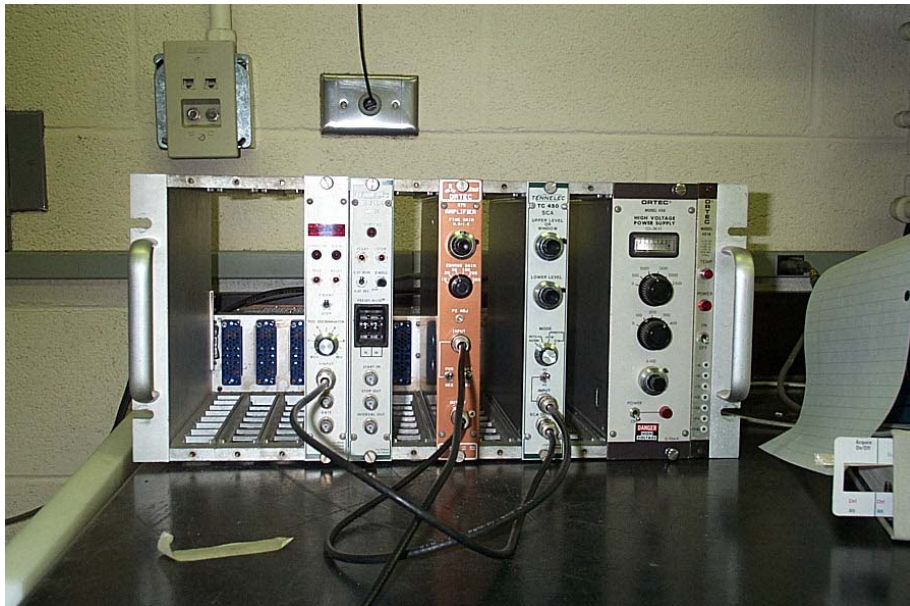


Figure B-1. Electronic apparatuses for experiment

APPENDIX C

Pictures For Sb(Be) Source Experiment



Figure C-1. Experimental device



Figure C-2. Aqueous Samples for experiment

APPENDIX D

Procedure for Test of A Sb(Be) Source

I. Source Description

The Sb(Be) pellet is contained by two welded stainless steel inner capsules which is placed inside a sealed, threaded aluminum outer capsule. The Sb(Be) pellet is held in place by tubing located inside the first stainless steel capsule. The aluminum outer capsule is sealed using a pipe thread sealant, e.g. Neolube from Huron Industries, Inc.

The Sb(Be) stainless steel capsule is to be activated periodically at the PULSTAR nuclear research reactor to produce up to 10 mCi of Sb-124. The irradiated capsule will then be placed in the threaded aluminum capsule sealed with a pipe thread sealant. Gamma photons emitted by Sb-124 interact with the Be to produce neutrons with a maximum emission rate of approximately 4000 n/s. The source will be periodically regenerated as needed since Sb-124 has a 60 day half-life. Source irradiation, use, testing, storage, shielding, and ALARA practices for the sealing of the aluminum outer capsule and source use will be followed as stated in applicable procedures and protocols.

II. Source Testing

Prior to the first activation of the source, the assembled Sb(Be) non-radioactive source, i.e. the stainless steel inner capsule placed inside the aluminum outer capsule, will be subjected to the following tests to verify integrity of the second stainless steel inner capsule:

1. Heat source in air at 80 °C for 1 hour, then allow the source to stand until ambient temperature is reached.
2. Place source in a freezer at -20 °C for 1 hour, then allow the source to stand until ambient temperature is reached.
3. Securely tape the source to a secured steel plate and allow a 50g mass of steel to freely strike the source from a distance of 1 m.
4. Drop the source from a distance of 1.5 m to a secured steel plate 10 times.
5. Place source in a 500 ml container. Place the container with the source in a wrist-action shaker for 30 minutes.

6. Drop a 10g steel mass on the edges of the second stainless steel inner capsule.
7. With the reactor shut down, seal the inner stainless steel source capsule in the outer aluminum capsule using a pipe thread sealant. Lower the assembled source to the bottom of the reactor pool (storage pit) and leave for 1 hour. Then, disassemble the source and observe for presence of water leaking from inside the second stainless steel inner capsule.
8. Perform a visual exam and note any physical defect(s) observed.
9. Ensure that the source is at ambient temperature and immerse the second stainless steel inner capsule in a water bath that is between 90 °C and 95 °C. Observe for bubble leaks over a period of at least 2 minutes.
10. If possible, radiograph the assembled source upon completion of leak testing.
11. Testing acceptance criteria are as follows:
 - a. If no physical defects are visible from step 8, the source is considered to be leak free.
 - b. If no bubbles are observed from step 9, the source is considered to be leak free.
 - c. If performed and no cracks or damage is observed by radiograph, the source is considered to be leak free.

NOTE: Test descriptions from ANSI/HPS N43.6-1997 were modified.

Refer to attached pages for testing results.

III. Source Use and Storage

- A. If radioactive, the Sb(Be) source will be used in the assembled form (inner stainless steel capsule placed and sealed inside the outer aluminum capsule) to perform and study neutron interactions for research projects and academic laboratories only in the Burlington Engineering Laboratories under protocol nos. 715, 716, or 724. Protocols 715 and 716 refer to applicable PULSTAR HP procedures for source activation and radiation safety requirements.
- B. If the source radioactivity exceeds 10 Ci, then perform leak testing after first irradiation and periodically thereafter as stated in procedure HP 7 and the broad scope university license.

INITIAL LEAK TEST RESULTS:

Prior to the first activation of the source, the assembled Sb(Be) non-radioactive source, i.e. the stainless steel capsules placed inside the aluminum outer capsule, will be subjected to the following tests to verify integrity of the second stainless steel inner capsule:

1. Heat source in air at 80 °C for 1 hour, then allow the source to stand until ambient temperature is reached.

(No visible defects observed upon completion of test.

2. Place source in a freezer at -20 °C for 1 hour, then allow the source to stand until ambient temperature is reached.

(No visible defects observed upon completion of test.

3. Securely tape the source to a secured steel plate and allow a 50g mass of steel to freely strike the source from a distance of 1 m.

(No visible defects observed upon completion of test other than minor scratches and dents to the outer aluminum capsule.

4. Drop the source from a distance of 1.5 m to a secured steel plate 10 times.

(No visible defects observed upon completion of test other than minor scratches and dents to the outer aluminum capsule..

5. Place source in a 500 ml container. Place the container with the source in a wrist-action shaker for 30 minutes.

(No visible defects observed upon completion of test.

6. Drop a 1g steel weight on the edges of the second stainless steel inner capsule.

(No visible defects observed upon completion of test.

7. With the reactor shut down, seal the inner stainless steel source capsule in the outer aluminum capsule using a pipe thread sealant. Lower the assembled source to the bottom of the reactor pool (storage pit) and leave for 1 hour. Then, disassemble the source and observe for presence of water leaking or seeping from inside the second stainless steel inner capsule.

(No water was observed leaking, dripping, or seeping from the inner stainless steel capsule upon completion of test. Water was observed inside the outer aluminum capsule.

8. Perform a visual exam and note any physical defect(s) observed. If no physical defects are observed, the source is considered to be leak free.

(No visible defects observed upon completion of the above tests.

9. Ensure that the source is at ambient temperature and immerse the second stainless steel inner capsule in a water bath that is between 90 °C and 95 °C. Observe for bubble leaks over a period of at least 2 minutes.

If no bubbles are observed, the source is considered to be leak free.

(No air bubbles were observed.

10. If possible, radiograph the assembled source upon completion of leak testing.

(Not performed at this time.

11. The following testing acceptance criteria were met:

(a. No physical defects were visible from step 8, the source is considered to be leak free.

(b. No bubbles were observed from step 9, the source is considered to be leak free.

NOTE: Test descriptions from ANSI/HPS N43.6-1997 were modified.

Per formed by: G. Wicks

Date: 4 April 2002

APPENDIX E PROCEDURE FOR USE OF A Sb(Be) SOURCE



Figure E-1. Outer Aluminum Capsule and End Caps (left) & Inner Stainless Steel (right) Capsule



Figure E-2. Outer Aluminum Capsule and End Caps (top) & Inner Stainless Steel (bottom) Capsule



Figure E-3. Figure E-3. End View of Inner Stainless Steel Capsule



Figure E-4. Assembled Source

APPENDIX F

Calculation for Source Mass

I. Density:

SS 304 : $\rho_{SS} = 8.027 \text{ g/cm}^3$

Antimony: $\rho_{Sb} = 6.68 \text{ g/cm}^3$

Beryllium: $\rho_{Be} = 1.85 \text{ g/cm}^3$

II. Mass:

1. Tube one (outer): $V_T^1 = \frac{\pi}{4} [(0.440")^2 - (0.355")^2] \times 3.130" = (0.166")^3$

Outer Plug: $V_P^1 = \frac{\pi}{4} (0.441")^2 \times 0.453" = (0.069")^3$

Mass one: $m^1 = \rho_{SS} (V_T^1 + 2V_P^1)$
 $= 8.027 \times (0.166 + 2 \times 0.069) \times (2.54 \text{ cm/in})^3$
 $= 39.988 \text{ g}$

2. Tube two (inner): $V_T^2 = \frac{\pi}{4} [(0.350")^2 - (0.257")^2] \times 2.343" = (0.104")^3$

Inner Plug: $V_P^2 = \frac{\pi}{4} (0.351")^2 \times 0.402" = (0.0389")^3$

Mass two: $m^2 = \rho_{SS} (V_T^2 + 2V_P^2)$
 $= 8.027 \times (0.104 + 2 \times 0.0389) \times (2.54 \text{ cm/in})^3$
 $= 23.914 \text{ g}$

3. Tube three (Approx.): $V_T^3 = \frac{\pi}{4} [(0.252")^2 - (0.189")^2] \times 1.4567" = (0.0318")^3$

Hollow Plug: $V_P^3 = \frac{\pi}{4} [(0.252")^2 - (0.189")^2] \times 1.4567" = (0.0318")^3$

Mass three: $m^3 = \rho_{SS} (V_T^3 + V_P^3)$
 $= 8.027 \times (0.0318 \times 0.01213) \times (2.54 \text{ cm/in})^3$
 $= 5.7785 \text{ g}$

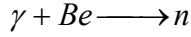
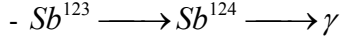
4. Pellet: $V_S = \frac{\pi}{4} (0.2632")^2 \times 0.627" = (0.0341")^3$

Mass source: $m_S = \frac{1}{2} V_S (\rho_{Sb} + \rho_{Be})$
 $= \frac{1}{2} \times (0.0341") \times (6.68 + 1.85) \times (2.54 \text{ cm/in})^3$
 $= 2.383 \text{ g}$

APPENDIX G

Calculation for Source Activation Time

I. Parameters.



Estimate Output: 4000 n/sec after 17 hours shutdown.

- Volume of Pellet: $V_{Sb} = \frac{\pi}{4} D^2 L = \frac{\pi}{4} (0.2632")^2 \times 0.627" = (0.0341")^3 = 0.559 cm^3$

- Microscopic activation cross-sections (thermal) for Sb^{123} : 1.107 barn
 Microscopic absorption cross-sections (2200 m/sec) for Sb^{124} : 6.5 barn

- Neutron Flux in Reactor : $\phi = 9.3 \times 10^{12}$ n/sec·cm² (Peak)

- Theoretical densities:

Antimony: $\rho_{Sb} = 6.68 g/cm^3$

Beryllium: $\rho_{Be} = 1.85 g/cm^3$

- Sb-Be combination: 50% by volume

- Antimony half-life : $T_{1/2} = 60$ days
 Decay constant of Sb^{124} : $\lambda_2 = 1.33 \times 10^{-7} sec^{-1}$
 Sb^{124} decay energy : $E = 2.916$ MeV

- Neutron self-shielding Factor: $F = 0.913$
 Hardening Factor : $H = 0.814$

II. Irradiation.

$$(II-1) \frac{dN_1}{dt} = -\phi\sigma_1 N_1$$

Where N_1 = number of atoms of Sb^{123}

ϕ = neutron flux

σ_1 = reaction cross-section of Sb^{123} for the formation of Sb^{124}

$$(II-2) N_1 = N_{10} \exp(-\phi\sigma_1 t)$$

$$(II-3) \frac{dN_2}{dt} = (\text{rate of production of } N^2) - (\text{rate of transmutation of } N^2) - (\text{rate of decay of } N^2)$$

$$= -\frac{dN_1}{dt} - \phi\sigma_2 N_2 - \lambda_2 N_2$$

$$= \phi\sigma_1 N_{10} \exp(-\phi\sigma_1 t) - (\phi\sigma_2 + \lambda_2) N_2$$

Where N_2 = number of atoms of Sb^{124}

σ_2 = capture cross-section of Sb^{124}

λ_2 = decay constant of Sb^{124}

$$(II-4) N_2 = \frac{\phi\sigma_1 N_{10}}{-\phi\sigma_1 + (\phi\sigma_2 + \lambda_2)} \{ \exp[-\phi\sigma_1 t] - \exp[-(\phi\sigma_2 + \lambda_2)t] \}$$

$$N_2 = \frac{A_2 \times 3.7 \times 10^{10} \text{ decay/sec} \cdot \text{Ci}}{\lambda_2}$$

Where A_2 = Activity of Sb^{124} at beginning of shutdown.

$$(II-5) P_0 = \alpha A_2$$

Where P_0 = number of neutrons per second at beginning of shutdown.

α = neutron yield per curie of Sb^{124} (5×10^5 n/sec·Ci)

$$(II-6) N_{10} = W_{\text{Sb}} \cdot N_A \cdot k / M_{\text{Sb}}$$

Where W_{Sb} = Initial weight of Sb of naturally-occurring isotopic distribution.

N_A = Avogadro's Number (6.022×10^{23} atoms/mole)

K = Fraction of Sb^{123} in naturally-occurring Sb (0.4275)

M_{Sb} = Atomic weight of naturally-occurring Sb (121.75 g/mole)

III. Shutdown (17 hours)

$$(III-1) A_S = A_2 \exp(-\lambda_2 t_S)$$

Where A_S = Activity of Sb^{124} after shutdown.

t_S = timeval for shutdown.

$$(III-2) P_S = P_0 \exp(-\lambda_2 t_S)$$

Where P_S = estimated neutron output per second (4000 n/sec).

IV. Calculation for activation time.

From equation (III-2),

$$\begin{aligned} P_S &= P_0 \exp(-\lambda_2 t_S) \\ &= 4000 \times \exp(1.33 \times 10^{-7} \times 17 \times 3600) \\ &= 4.0327 \times 10^3 \text{ n/sec} \end{aligned}$$

From equation (II-5),

$$A_2 = \frac{P_0}{\alpha} = \frac{4.0327 \times 10^3 \text{ n/sec}}{5 \times 10^5 \text{ n/sec} \cdot \text{Ci}} = 8.0654 \times 10^{-3} \text{ Ci} = 8.0654 \text{ mCi}$$

From equation (II-4),

$$\begin{aligned} N_2 &= \frac{A_2 \times 3.7 \times 10^{10} \text{ decay/sec} \cdot \text{Ci}}{\lambda_2} \\ &= \frac{8.0654 \times 10^{-3} \times 3.7 \times 10^{10}}{1.33 \times 10^{-7}} \\ &= 2.2438 \times 10^{15} \end{aligned}$$

$$\phi\sigma_1 = 9.3 \times 10^{12} \times 1.107 \times 10^{-24} \times 0.913 = 9.3994 \times 10^{-12} \text{ /sec} \cdot \text{atom}$$

$$\phi\sigma_2 = 9.3 \times 10^{12} \times 6.5 \times 10^{-24} \times 0.913 \times 0.814 = 4.4925 \times 10^{-11} \text{ /sec} \cdot \text{atom}$$

From equation (II-6),

$$\begin{aligned}
 W_{Sb} &= V_{Pellet} \cdot 50\% \cdot \rho_{Sb} \\
 &= 0.559 \times 0.5 \times 6.68 = 1.867 \text{ g} \\
 N_{10} &= W_{Sb} \cdot N_A \cdot k / M_{Sb} \\
 &= \frac{1.867 \text{ g} \times 6.0225 \times 10^{23} \text{ atoms / mole} \times 0.4275}{121.75 \text{ g / mole}} \\
 &= 3.9481 \times 10^{21}
 \end{aligned}$$

From Matlab, activation time is(Fig-1A):

$$t = 5.54 \times 10^4 \text{ sec} = 15.38 \text{ hours}$$